Environmental Science & Technology Letters

pubs.acs.org/journal/estlcu

Letter

Occurrences of Tire Rubber-Derived Contaminants in Cold-Climate Urban Runoff

J. K. Challis, H. Popick, S. Prajapati, P. Harder, J. P. Giesy, K. McPhedran, and M. Brinkmann*

Cite This: *Environ. Sci. Technol. Lett.* 2021, 8, 961−967

Read Online

ACCESS | Metrics & More | Article Recommendations | Supporting Information

ABSTRACT: Recent findings that 2-anilo-5-[(4-methylpentan-2-yl)amino]cyclohexa-2,5-diene-1,4-dione (6PPD-quinone), the transformation product of a common tire rubber antioxidant, is acutely toxic in stormwater-impacted streams has highlighted the need for a better understanding of contaminants in urban runoff. This study represents one of the first reports of 6PPD-quinone and other tire rubber-derived compounds in stormwater and snowmelt of a cold-climate Canadian city (Saskatoon, 2019−2020). Semiquantification of the five target compounds, N,N′-diphenylguanidine (DPG), N,N-dicyclohexylmethylamine (DCA), N,N′-dicyclohexylurea (DCU), 1-cyclohexyl-3-phenylurea (CPU), and 6PPD-quinone, revealed DPG was most abundant, with average concentrations of 60 μg L^{-1} in stormwater and 1 μg L^{-1} in snowmelt. Maximum observed concentrations of DPG were greater than 300 μg L^{-1}, equivalent to loadings of 15 kg from a single rain event. These concentrations of DPG represent some of the highest reported in urban runoff globally. 6PPD-Quinone was detected in 57% (12/21) of stormwater samples with a mean concentration of approximately 600 ng L^{-1} (2019) and greater than 80% (28/31) of snowmelt samples with mean concentrations of 80−370 ng L^{-1} (2019 and 2020). Concentrations of 6PPD-quinone exceeded the acute LC_{50} for coho salmon (0.8−1.2 μg L^{-1}) in greater than 20% of stormwater samples. Mass loadings of all target chemicals correlated well with roads and residential land-use area.

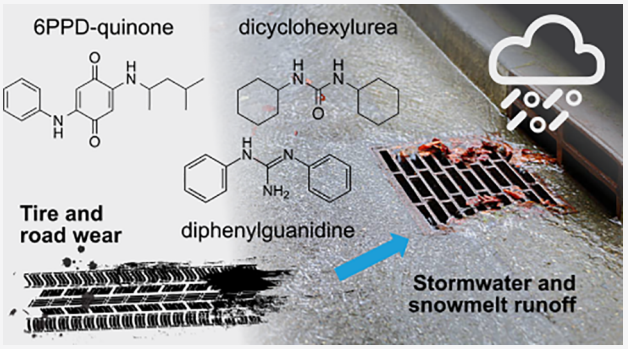

INTRODUCTION

Stormwater and snowmelt runoff represent important and complex sources of chemical mixtures entering surface waters. In urbanized environments, runoff events can mobilize nutrients, road salts, and many inorganic and organic contaminants.[1−3] Urbanization has resulted in greater quantities and lesser quality of surface runoff, posing challenges for protection of municipal infrastructure and receiving environments. Additionally, the diffuse and often stochastic nature of urban runoff makes the sampling of these complex mixtures difficult.[1−3] Recently, nontarget analysis using high-resolution mass spectrometry (HRMS) has been employed to characterize urban runoff beyond this typical suite of targeted analytes (e.g., metals, polycyclic aromatic hydrocarbons).[4−13] Common among these studies was ubiquitous detection of compounds related to manufacturing of tire rubber and plastics, including bicyclic amines and melamine derivatives, frequently measured at concentrations of μg L^{-1} in urban runoff[7,13] and even surface waters during precipitation events.[14]

Multiple studies have reported toxic potency of tire rubber leachate to algae,[15] anthropods,[16] molluscs,[15] fish,[17−19] and vertebrate embryos.[20] The rubber vulcanizing agent, N,N′-diphenylguanidine (DPG) has been reported to be a highly abundant feature identified by nontarget analysis in road runoff.[7,13] DPG has measured acute (48 h LC_{50}) and chronic (21 day) toxicities of 17 and 0.6 mg L^{-1} (daphnia).[21] The recent discovery that the tire rubber-derived transformation product 2-anilo-5-[(4-methylpentan-2-yl)amino]cyclohexa-2,5-diene-1,4-dione (6PPD-quinone) is the primary causal toxicant for urban runoff mortality syndrome affecting Pacific Northwest coho salmon[9] has brought significant attention to this source of contamination. Further confounding this issue are efforts toward recycling and utilization of scrap tire material. For example, in 2009, scrap tire material generated in the U.S. exceeded 4.5 billion kg, with greater than 80% of that being utilized in the scrap tire market.[22] Uses include sporting and playground surfaces, mulch, septic field drainage, and recycled construction materials, including asphalt concrete made with recycled crumb rubber, in some cases, without a comprehensive consideration for, or assessment of potential environmental impacts.[22−26]

Received: August 23, 2021
Revised: September 16, 2021
Accepted: September 17, 2021
Published: September 22, 2021

Downloaded via UNIV OF SASKATCHEWAN on December 10, 2021 at 19:00:47 (UTC).
See https://pubs.acs.org/sharingguidelines for options on how to legitimately share published articles.

ACS Publications

© 2021 The Authors. Published by American Chemical Society

This study reports occurrences of five compounds derived from tire rubber, including the recently discovered transformation product 6PPD-quinone, in stormwater and snowmelt runoff in the semiarid, cold-climate city of Saskatoon, Saskatchewan, Canada.

MATERIALS AND METHODS

Chemical Standards. Chemical standards N,N′-diphenylguanidine (DPG), N,N-dicyclohexylmethylamine (DCA), N,N′-dicyclohexylurea (DCU), and 1-cyclohexyl-3-phenylurea (CPU) were purchased from Sigma-Aldrich (Oakville, ON). The 2-anilo-5-[(4-methylpentan-2-yl)amino]cyclohexa-2,5-diene-1,4-dione (6PPD-quinone) standard was kindly provided by Dr. Kolodziej's research group who identified, synthesized, and purified this compound.[9] Native and isotopically labeled 6PPD-quinone-(d5) was purchased from Toronto Research Chemicals, Toronto, ON. See Supporting Information, Section 1.1, for complete chemical standard and reagent details.

Study Region and Sampling Sites. The City of Saskatoon (City) is the largest municipality in Saskatchewan with a population of approximately 330,000 covering an area of 140 km^2. The Saskatoon climate is classified as warm humid continental (Dfb) according to the Köppen−Geiger classification system with an average annual precipitation of 465 mm and approximately 50% of that falling as rainfall in June, July, and August. The City has more than 100 stormwater outfalls, some of which are connected to a network of treatment ponds, while others are discharged directly into the South Saskatchewan River (SSR). The City also has four snow dump sites for managing winter precipitation. Snowmelt samples were collected between March and May of 2019 and 2020 at four City snow dumps (Supporting Information, Figure S1). Snow from the piles was collected from 8 to 12 random locations on the surfaces and sides of the snow piles and combined in a 25 L container (Supporting Information, Section 1.2.2). Stormwater was collected in June, July, and August, 2019 (Supporting Information, B2) at seven outfalls along the SSR representing a mix of residential, industrial, and retail developments (Supporting Information, Section 1.2.1, Supporting Information, B1).[27] River water samples were also taken from nine SSR sites on one date in each of June, August, and October 2020 (Supporting Information, Figure S2). Only a single SSR site (Downtown) falls inside the City limits. Field and lab blanks containing Milli-Q water were acquired for each sampling event. The target analytes were below limits of detection in all blanks.

Sample Extraction and Processing. Stormwater, snowmelt, river samples, and lab and field blanks were filtered through Whatman GF/F glass microfiber filters (0.7 μm) and extracted using Oasis HLB solid-phase extraction cartridges prior to analysis. Complete details of the extraction protocols are found in Supporting Information, Section 1.2.4.

Instrumental Analysis. Analysis was conducted using a Vanquish UHPLC and Q-Exactive HF Quadrupole-Orbitrap mass spectrometer (Thermo-Fisher, Mississauga, ON). LC separation was achieved with a Kinetex 1.7 μm XB-C18-LC column (100 mm × 2.1 mm) (Phenomenex, Torrance, CA) by gradient elution (Supporting Information, Tables S3 and S4) with water and methanol, both containing 0.1% formic acid at a flow rate of 0.2 mL min^{-1} and column temperature of 40 °C. Method detection limits ranged from 0.3−1.2 ng mL^{-1} (Supporting Information, Table S6). All MS method details including precursor/product ions (Supporting Information, Table S5) and example chromatographs and MS spectra (Supporting Information, Figures S3−S7) can be found in the Supporting Information, Section 1.3. Suspect screening was conducted using Compound Discoverer 2.1 (Supporting Information, Figures S8 and S9), and targeted semiquantification was done with TraceFinder 4.1 (ThermoFisher Scientific).

Semiquantification of Target Compounds. The suspect screening analyses tentatively identified N,N′-diphenylguanidine (DPG), N,N-dicyclohexylmethylamine (DCA), N,N′-dicyclohexylurea (DCU), and 1-cyclohexyl-3-phenylurea (CPU) in the storm runoff and snowmelt samples. These four bicyclic amines are associated with tire rubber manufacturing and have been detected in tire rubber leachate,[28] and road runoff.[7,13] These four compounds also had readily available authentic standards. Additionally, following its recent discovery as a toxic stormwater contaminant,[9] the transformation product 6PPD-quinone was included in the targeted method. These five tire rubber-derived contaminants were retrospectively confirmed by comparison of retention times, accurate masses, and mass fragments to authentic analytical standards. Semiquantification was done using a targeted external calibration method, which based on extraction efficiencies and matrix effects data (Supporting Information, Tables S7−S9) may be underestimated by a factor of 2 or more (Supporting Information, Section 2.2).

RESULTS AND DISCUSSION

Snowmelt. Concentrations of all five target compounds were detected with varying frequencies in snowmelt from 2019 and 2020 (Supporting Information, Table S10 and Figure S10, and Supporting Information, B4). Concentrations of 6PPD-quinone, DCA, and CPU were consistently greater in snowmelt samples from 2019 compared to 2020, by on average 2−8-fold. This yearly trend was less clear for DPG, skewed by a single high concentration in 2020 (8667 ng L^{-1}), and DCU which had a low detection frequency in 2019 (20%). Approximately 35% more snow accumulated in Saskatoon in 2019 versus 2020, potentially influencing concentrations for some of the tire rubber-derived compounds in City snow dumps. Additionally, 2019 samples were snow melted in the lab, while 2020 samples were collected as snowmelt on site. This, and other factors, including age of snow prior to sampling (e.g., compound degradation), frequency of snow clearing, dilution from fresh snow fall, and rate of melting, could be confounding these observations.[27,29,30] Snow samples were taken as composites from 8 to 12 locations representing both new and old snow. Therefore, these samples are not appropriate for a detailed elucidation of fate mechanisms occurring in the snow dump or during melt events. Assuming measured chemical concentrations from Valley Road snow (Supporting Information, Table S10) are representative of the entire snow dump, mass loading estimates are 10 g of 6PPD-quinone, 150 g of DPG, 0.3 g of DCA, 2 g of DCU, and 0.4 g of CPU (Supporting Information, Section 2.4).

Stormwater Concentrations. Sampling of stormwater took place in 2019 across seven sites (Supporting Information, Figure S1) and four sampling events between June and August. Each sampling event typically took place within hours of the onset of a precipitation event with the exception of the July 24−25 event which took place approximately 24 h later (Supporting Information, B2). Concentrations of all target compounds were on average 3−60-fold greater in stormwater

https://doi.org/10.1021/acs.estlett.1c00682
Environ. Sci. Technol. Lett. 2021, 8, 961−967

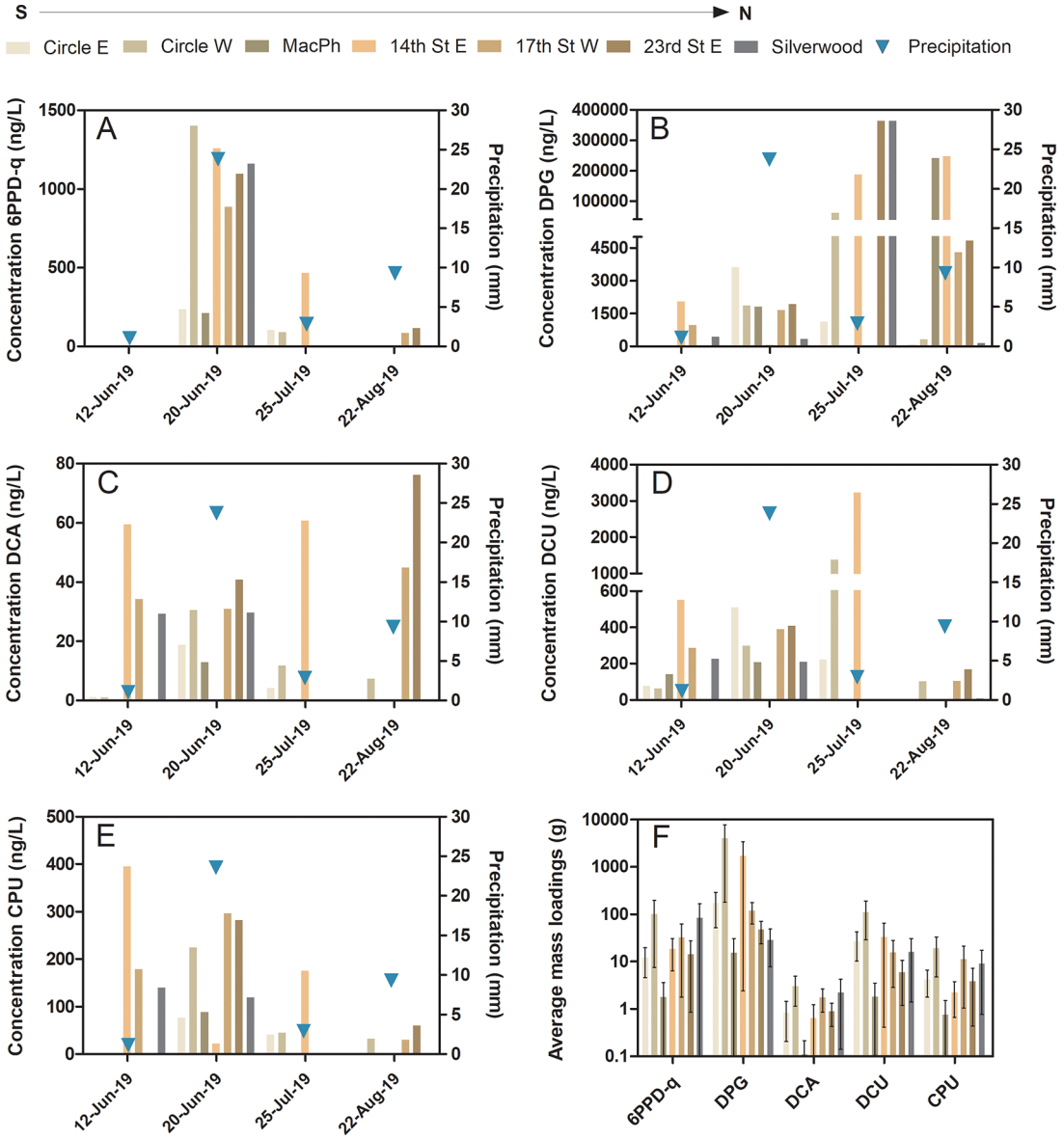

Figure 1. Concentrations (ng L^{-1}) of 6PPD-quinone (A), N,N′-diphenylguanidine (DPG) (B), N,N-dicyclohexylmethylamine (DCA) (C), N,N′-Dicyclohexylurea (DCU) (D), and 1-cyclohexyl-3-phenylurea (CPU) (E) in stormwater samples from 2019 with precipitation events (mm) overlaid. Each bar in A–E represents a single sample. Mass loadings in (F) are the average (±standard error) across all dates at each sampling site (note log scale). Sampling locations correspond to street names in closest proximity to stormwater outfalls (see map in Figure S1).

as compared to snowmelt, a result indicative of the greater maximum concentrations observed during storm runoff events compared to the composite snowmelt samples.

Comparing the June 20, July 25, and August 22 sampling events and resulting compound concentrations (Figure 1, Supporting Information, Table S11 and B3) highlights some of the confounding factors related to studying stormwater runoff. June 20 and August 22 saw single large rain events (24 and 10 mm, respectively, Supporting Information, B2) preceded by multiple days of dry conditions (<0.4 mm), whereas July 25 saw a relatively small amount of rainfall (2.9 mm) on the day of sampling but was preceded by 19.2 mm of rain the day prior (July 24) (Supporting Information, B2). Maximum concentrations of DPG were observed at multiple sites on both July 25 (61–364 μg L^{-1}) and August 22 (242–248 μg L^{-1}), whereas DPG concentrations were less than 4 μg L^{-1} on June 20. The maximum observed DPG concentrations observed on July 25, nearly 18 h after the start of the July 24 event (19.2 mm, Supporting Information, B2), are somewhat surprising given that lag times to peak concentrations in direct runoff are expected to be much less than lag times previously reported in receiving waters (12–18 h).[12,14] These findings suggest that the elevated DPG concentrations either represent the tail end of the chemograph and missed peak concentrations were in fact much higher (i.e., mg L^{-1} range) or this large flush event produced elevated DPG levels over an extended period of time. In contrast, the lower concentrations of DPG observed on June 20 (sampled approximately 9 h into the rain event, Supporting Information, B2) may indicate the contaminant peak was missed. However, a major influence here may relate to street cleaning, which is typically done in May, and could have led to reduced concentrations in June.

All four bicyclic amines (excluding the exceptionally high DPG concentrations at two sites on July 25 and on August 22)

https://doi.org/10.1021/acs.estlett.1c00682
Environ. Sci. Technol. Lett. 2021, 8, 961–967

share similar concentration profiles across sampling dates and sites (Figure 1B−E). In contrast, 6PPD-quinone showed maximum observed concentrations across most sites on June 20 and only select detections on July 25 and August 22 (Figure 1A). Reasons for the observed differences are not clear; however, the sources, fate, and transport dynamics of these compounds are likely playing roles. The transformation product 6PPD-quinone is generated via ozonation of the common tire rubber antioxidant 6PPD,[9] whereas DPG, for example, is expected to leach directly from car tires (i.e., no transformation) and has multiple other industrial applications including use in rubber gloves, footwear, hosing, and cables.[21] To what extent these other sources are contributing to DPG levels is not known at this time; however, we still expect car tires to be by far the major source of DPG in this study.

Recent reports of these compounds in storm runoff and receiving systems come from the heavily urbanized and densely populated Seattle, WA, USA[8] and Toronto, ON, Canada.[31] While population in these regions differ significantly (≈270,000 Saskatoon versus ≈4,000,000 Seattle and ≈6,300,000 Toronto), estimated densities are more comparable (Saskatoon ≈1900 versus Seattle ≈3100 and Toronto ≈4300 persons/km^2). Average concentrations of 10, 300, and 350 ng L^{-1} DCA, DCU, and CPU in Seattle stormwater runoff[13] are comparable to means observed during the present study of 30, 450, and 130 ng L^{-1} DCA, DCU, and CPU, respectively (Supporting Information, Table S11 and B3). However, the mean concentration of 1.8 μg L^{-1} DPG reported in road runoff in the same study[13] was approximately 30-fold less than that observed here (≈60 μg L^{-1}). Concentrations of DPG measured in a small Toronto creek and river ranged from 0.16−0.76 μg L^{-1} during two summer rain events.[31] These concentrations are approximately 80- to 400-fold less than our reported stormwater runoff concentrations, a result attributed to in-stream dilution.

Sampling at 10 South Saskatchewan River sites revealed that of the five target compounds only DPG was measured at detectable levels (Supporting Information, Table S12), allowing for a comparison of surface water concentrations with the Toronto study. DPG was detected in 100% (n = 26) of river samples at 24 ± 76 ng L^{-1} (range = 0.7−401 ng L^{-1}), which agrees well with reported surface water concentrations elsewhere[12,13] but is greater than 20-fold less than those reported in Toronto surface waters.[31] This is consistent with average discharges of 1−4 m^3 s^{-1} in the Don River and Highland Creek,[31] which are 50−100-fold less than average flows in the South Saskatchewan River (≈200 m^3 s^{-1}). Accounting for in-stream dilution in this way would suggest that concentrations of DPG in direct stormwater runoff in Toronto would be similar to the elevated levels found in Saskatoon. Regardless, with maximum observed concentrations greater than 300 μg L^{-1}, to our knowledge these represent some of the highest concentrations of DPG observed in stormwater runoff globally.

Reasons for these exceptionally high concentrations are not known; however, it may relate to the climate, characterized by occasional but intense rainstorms often preceded and/or followed by extended dry periods. Months-long winters are characterized by dramatic temperature fluctuations (seasonal and daily) and low absolute humidity, potentially aggravating mechanical degradation processes of tires and roads.[32,33] These conditions can lead to significant accumulation and subsequent flushing of tire rubber material from roads during rainfall events. Other factors unique to cold-climate regions that may be contributing to these elevated levels include poor road conditions (i.e., potholes), the widespread use of softer-rubber winter tires,[34−36] and application of sand and salt to roads. One report measuring tire wear particles found that concentrations of PM_{10} generated from winter tires and studded winter tires were approximately 10- and 100-fold greater compared to summer tires, respectively.[35] The widespread use of winter tires in Saskatoon and the fact that there are no restrictions on studded tires in the province may be contributing to these high DPG concentrations.

Concentrations of 6PPD-quinone in stormwater runoff ranged from 86−1400 ng L^{-1} with a detection frequency of 57% (12/21) across all sites and sampling events (Figure 1, Supporting Information, Table S11 and B3). Tian et al. observed an average 6PPD-quinone concentration of 7000 ± 4500 ng L^{-1} in roadway runoff from two sites (n = 16),[9] which is approximately 10-fold greater than the average concentration observed here (593 ± 525 ng L^{-1}). Johannessen et al. reported concentrations of 210−720 ng L^{-1} 6PPD-quinone in the same Toronto surface waters discussed above,[31] with likely concentrations in direct runoff (no in-stream dilution) to be much greater. The reported LC_{50} of 6PPD-quinone to coho salmon is 800−1200 ng L^{-1}, meaning that 5 of 12 sampling events where 6PPD-quinone was detected would exceed this LC_{50}. While coho salmon are not found in the South Saskatchewan River, risks of 6PPD-quinone exposure to other species of fishes (e.g., northern pike, lake trout) and other aquatic organisms are currently unknown.

Stormwater Loadings. Stormwater runoff volumes were estimated based on precipitation depth corresponding to each sampling event, catchment area, and land-use data obtained from the City of Saskatoon.[37] Specifically, a stormwater volume was calculated for each land-use (LU) area (Supporting Information, B1) comprising a single sampling catchment ($CR_{LU} \times A_{LU} \times P$) and then summed to obtain the total stormwater runoff volume for that catchment for each precipitation event (Supporting Information, B2). These data were used to estimate chemical loadings (eq 1).

$$L = \left(\sum CR_{LU} \times A_{LU}\right) \times P \times C \quad (1)$$

where L (kg) is the chemical load, $CR_{LU} \times A_{LU}$ (km^2) the dimensionless land-use specific runoff coefficient and land-use specific area, respectively, summed together for a total land-use specific stormwater catchment area, P the event precipitation depth (mm), and C the chemical concentration measured at a specific stormwater outfall on a given sampling day. Measured concentrations were assumed to be constant over the duration of each rainfall event, potentially leading to over- or underestimations of loadings. As such, the reported mass loadings should be considered qualitative estimates.

Average loadings of 6PPD-quinone, DCA, DCU, and CPU across all sites and dates ranged from 1−50 g per rainfall event, whereas average DPG loadings exceeded 1 kg and reached approximately 15 kg maximally, from a single rain event (July 25, Circle W sampling site) (Figure 1F, Supporting Information, Figure S12 and B3). A recent study in urban streams around Toronto, Ontario, Canada reported 6PPD-quinone loadings of 34 and 416 g during a heavy August rainfall (25 mm),[31] consistent with mass loadings of 1.7−384 g observed here. The same study reported DPG loadings of 26 and 454 g during this same storm event, significantly less than

https://doi.org/10.1021/acs.estlett.1c00682
Environ. Sci. Technol. Lett. 2021, 8, 961−967

our calculated DPG loadings (Figure 1F and Supporting Information, B3). The mass loads of DPG reported here are more comparable with HMMM (0.09−13 kg/event)[14] and total HMMM (HMMM + transformation products) (2.8−25 kg/event)[31] measured in the Don River and Highland Creek, Toronto, Ontario, Canada. It should be noted that loading calculations discussed above from Johannessen et al.[14,31] are based on in-stream samples over the course of a storm event, providing greater temporal resolution and accuracy than accomplished here and, thus, are not directly comparable to our stormwater outfall samples.

Land-Use Correlations. Spatial and temporal trends of the target compounds (Figure 1) as a function of precipitation events and antecedent dry periods were not observed, possibly due to the small sample size (2−4 sampling events per site) and other confounding sampling factors (e.g., lag times[12,14]). However, linear regression analysis of mass loadings as a function of land-use area (land-use definitions and breakdowns in Supporting Information, B1) at each of the seven sampling sites indicate strong positive correlations with roads (average r^2 = 0.800) and residential areas (average r^2 = 0.883) and no correlations with industrial areas and green spaces (Table S13). Hou et al. also observed greater surface water concentrations of vehicle-related chemicals (e.g., HMMM, DPG) in areas of higher traffic density. In the current study, DPG demonstrated poorer correlations with roads (r^2 = 0.576) and residential (r^2 = 0.734) areas compared to the other four compounds (r^2 > 0.753 roads and r^2 > 0.844 residential). This may suggest multiple important sources of DPG contributing to the observed levels; however, this requires further research to confirm.

The findings of this study highlight important differences in the occurrences of tire rubber-derived compounds, in particular DPG, when compared across studies conducted in different geographies. While the reasons for these differences are not completely clear at this time, we suspect it is a combination of factors related to land-use, infrastructure, population, climate, study sampling design, and chemical transport dynamics. Future studies should be designed with the purpose of delineating the impact of these variables on the occurrence and fate of stormwater-related compounds.

■ ASSOCIATED CONTENT

Supporting Information

The Supporting Information is available free of charge at https://pubs.acs.org/doi/10.1021/acs.estlett.1c00682.

Maps and sampling details, instrumental and data analysis details, chromatographic peaks and mass spectra, detection limits, stormwater and snowmelt concentrations (PDF)

B1: Land-use data and runoff coefficients used for loading calculations. B2: Precipitation events and sampling time. B3: Stormwater concentrations and loadings. B4: Snowmelt concentrations (XLSX)

■ AUTHOR INFORMATION

Corresponding Author

M. Brinkmann − *Toxicology Centre, University of Saskatchewan, Saskatoon, SK, Canada S7N 5B3; School of Environment and Sustainability, University of Saskatchewan, Saskatoon, SK, Canada S7N 5C8; Global Institute for Water Security, University of Saskatchewan, Saskatoon, SK, Canada S7N 3H5;* orcid.org/0000-0002-4985-263X; Email: markus.brinkmann@usask.ca

Authors

J. K. Challis − *Toxicology Centre, University of Saskatchewan, Saskatoon, SK, Canada S7N 5B3;* orcid.org/0000-0003-3514-0647

H. Popick − *Department of Civil, Geological, and Environmental Engineering, College of Engineering, University of Saskatchewan, Saskatoon, SK, Canada S7N 5A9*

S. Prajapati − *School of Environment and Sustainability, University of Saskatchewan, Saskatoon, SK, Canada S7N 5C8*

P. Harder − *Centre for Hydrology, University of Saskatchewan, Saskatoon, SK, Canada S7N 1K2; Global Institute for Water Security, University of Saskatchewan, Saskatoon, SK, Canada S7N 3H5*

J. P. Giesy − *Toxicology Centre, University of Saskatchewan, Saskatoon, SK, Canada S7N 5B3; Department of Veterinary Biomedical Sciences, University of Saskatchewan, Saskatoon, SK, Canada S7N 5B4; Department of Environmental Science, Baylor University, Waco, Texas 76706, United States; Global Institute for Water Security, University of Saskatchewan, Saskatoon, SK, Canada S7N 3H5*

K. McPhedran − *Department of Civil, Geological, and Environmental Engineering, College of Engineering, University of Saskatchewan, Saskatoon, SK, Canada S7N 5A9*

Complete contact information is available at: https://pubs.acs.org/10.1021/acs.estlett.1c00682

Author Contributions

J. K. Challis and H. Popick contributed equally to this research and share first authorship.

Notes

The authors declare no competing financial interest.

■ ACKNOWLEDGMENTS

The authors thank Dr. Kolodziej and Dr. Tian for providing the 6PPD-quinone standard used to confirm our identifications and quantify 6PPD-quinone concentrations. The authors thank S. Rutley for assistance with map making. The authors thank Dr. John Pomeroy for facilitating access to the UAS-lidar system through the Smart Water Systems Laboratory. J. K. Challis was supported by a Banting postdoctoral fellowship. This research was conducted in partnership with the City of Saskatoon and funded through the ENGAGE program of the Natural Sciences and Engineering Research Council of Canada (NSERC). M. Brinkmann is currently a faculty member of the Global Water Futures program, which is funded through the Canada First Research Excellence Fund (CFREF). J. P. Giesy was supported by the Canada Research Chair program and a Distinguished Visiting Professorship in the Department of Environmental Sciences, Baylor University in Waco, TX, USA. The research was supported, in part, by a Discovery Grant from the Natural Science and Engineering Research Council of Canada (326415-07) and a grant from the Western Economic Diversification Canada (6578, 6807, and 000012711). The authors wish to acknowledge the support of an instrumentation grant from the Canada Foundation for Infrastructure and is part of the project titled "Next generation solutions to ensure healthy water resources for future generations" funded by the Global Water Futures program, Canada First Research

Excellence Fund. Additional information is available at www.globalwaterfutures.ca.

REFERENCES

(1) Zgheib, S.; Moilleron, R.; Chebbo, G. Priority Pollutants in Urban Stormwater: Part 1 - Case of Separate Storm Sewers. *Water Res.* **2012**, *46* (20), 6683−6692.

(2) Gasperi, J.; Zgheib, S.; Cladière, M.; Rocher, V.; Moilleron, R.; Chebbo, G. Priority Pollutants in Urban Stormwater: Part 2 - Case of Combined Sewers. *Water Res.* **2012**, *46* (20), 6693−6703.

(3) Masoner, J. R.; Kolpin, D. W.; Cozzarelli, I. M.; Barber, L. B.; Burden, D. S.; Foreman, W. T.; Forshay, K. J.; Furlong, E. T.; Groves, J. F.; Hladik, M. L.; Hopton, M. E.; Jaeschke, J. B.; Keefe, H.; Krabbenhoft, D. P.; Lowrance, R.; Romanok, K. M.; Rus, D. L.; Selbig, W. R.; Williams, B. H.; Bradley, P. M. Urban Stormwater: An Overlooked Pathway of Extensive Mixed Contaminants to Surface and Groundwaters in the United States. *Environ. Sci. Technol.* **2019**, *53*, 10070−10081.

(4) Carpenter, C. M. G.; Wong, L. Y. J.; Johnson, C. A.; Helbling, D. E. Fall Creek Monitoring Station: Highly Resolved Temporal Sampling to Prioritize the Identification of Nontarget Micropollutants in a Small Stream. *Environ. Sci. Technol.* **2019**, *53*, 77−87.

(5) Alhelou, R.; Seiwert, B.; Reemtsma, T. Hexamethoxymethylmelamine - A Precursor of Persistent and Mobile Contaminants in Municipal Wastewater and the Water Cycle. *Water Res.* **2019**, *165*, 114973.

(6) Seiwert, B.; Klöckner, P.; Wagner, S.; Reemtsma, T. Source-Related Smart Suspect Screening in the Aqueous Environment : Search for Tire-Derived Persistent and Mobile Trace Organic Contaminants in Surface Waters. *Anal. Bioanal. Chem.* **2020**, *412*, 4909−4919.

(7) Du, B.; Tian, Z.; Peter, K. T.; Kolodziej, E. P.; Wong, C. S. Developing Unique Nontarget High-Resolution Mass Spectrometry Signatures to Track Contaminant Sources in Urban Waters. *Environ. Sci. Technol. Lett.* **2020**, *7* (12), 923−930.

(8) Tian, Z.; Peter, K. T.; Gipe, A. D.; Zhao, H.; Hou, F.; Wark, D. A.; Khangaonkar, T.; Kolodziej, E. P.; James, C. A. Suspect and Nontarget Screening for Contaminants of Emerging Concern in an Urban Estuary. *Environ. Sci. Technol.* **2020**, *54* (2), 889−901.

(9) Tian, Z.; Zhao, H.; Peter, K. T.; Gonzalez, M.; Wetzel, J.; Wu, C.; Hu, X.; Prat, J.; Mudrock, E.; Hettinger, R.; Cortina, A. E.; Biswas, R. G.; Kock, F. V. C.; Soong, R.; Jenne, A.; Du, B.; Hou, F.; He, H.; Lundeen, R.; Gilbreath, A.; Sutton, R.; Scholz, N.; Davis, J.; Dodd, M. C.; Simpson, A.; McIntyre, J. K.; Kolodziej, E. P. A Ubiquitous Tire Rubber−Derived Chemical Induces Acute Mortality in Coho Salmon. *Science (Washington, DC, U. S.)* **2021**, *371* (6525), 185−189.

(10) Peter, K. T.; Wu, C.; Tian, Z.; Kolodziej, E. P. Application of Nontarget High Resolution Mass Spectrometry Data to Quantitative Source Apportionment. *Environ. Sci. Technol.* **2019**, *53* (21), 12257−12268.

(11) Overdahl, K. E.; Sutton, R.; Sun, J.; DeStefano, N. J.; Getzinger, G. J.; Ferguson, P. L. Assessment of Emerging Polar Organic Pollutants Linked to Contaminant Pathways within an Urban Estuary Using Non-Targeted Analysis. *Environ. Sci. Process. Impacts* **2021**, *23*, 429.

(12) Peter, K. T.; Hou, F.; Tian, Z.; Wu, C.; Goehring, M.; Liu, F.; Kolodziej, E. P. More Than a First Flush: Urban Creek Storm Hydrographs Demonstrate Broad Contaminant Pollutographs. *Environ. Sci. Technol.* **2020**, *54* (10), 6152−6165.

(13) Peter, K. T.; Tian, Z.; Wu, C.; Lin, P.; White, S.; Du, B.; McIntyre, J. K.; Scholz, N. L.; Kolodziej, E. P. Using High-Resolution Mass Spectrometry to Identify Organic Contaminants Linked to Urban Stormwater Mortality Syndrome in Coho Salmon. *Environ. Sci. Technol.* **2018**, *52* (18), 10317−10327.

(14) Johannessen, C.; Helm, P.; Metcalfe, C. D. Runoff of the Tire-Wear Compound, Hexamethoxymethyl-Melamine into Urban Watersheds. *Arch. Environ. Contam. Toxicol.* **2021**, *1*, na DOI: 10.1007/s00244-021-00815-5.

(15) Capolupo, M.; Sørensen, L.; Jayasena, K. D. R.; Booth, A. M.; Fabbri, E. Chemical Composition and Ecotoxicity of Plastic and Car Tire Rubber Leachates to Aquatic Organisms. *Water Res.* **2020**, *169*, 115270.

(16) Halsband, C.; Sørensen, L.; Booth, A. M.; Herzke, D. Car Tire Crumb Rubber: Does Leaching Produce a Toxic Chemical Cocktail in Coastal Marine Systems? *Front. Environ. Sci.* **2020**, *8* (July), 1−15.

(17) Stephensen, E.; Adolfsson-Erici, M.; Hulander, M.; Parkkonen, J.; Förlin, L. Rubber Additives Induce Oxidative Stress in Rainbow Trout. *Aquat. Toxicol.* **2005**, *75* (2), 136−143.

(18) LaPlaca, S. B.; van den Hurk, P. Toxicological Effects of Micronized Tire Crumb Rubber on Mummichog (Fundulus Heteroclitus) and Fathead Minnow (Pimephales Promelas). *Ecotoxicology* **2020**, *29* (5), 524−534.

(19) Kolomijeca, A.; Parrott, J.; Khan, H.; Shires, K.; Clarence, S.; Sullivan, C.; Chibwe, L.; Sinton, D.; Rochman, C. M. Increased Temperature and Turbulence Alter the Effects of Leachates from Tire Particles on Fathead Minnow (Pimephales Promelas). *Environ. Sci. Technol.* **2020**, *54*, 1750−1759.

(20) Xu, E. G.; Lin, N.; Cheong, R. S.; Ridsdale, C.; Tahara, R.; Du, T. Y.; Das, D.; Zhu, J.; Pena Silva, L.; Azimzada, A.; Larsson, H. C. E.; Tufenkji, N. Artificial Turf Infill Associated with Systematic Toxicity in an Amniote Vertebrate. *Proc. Natl. Acad. Sci. U. S. A.* **2019**, *116* (50), 25156−25161.

(21) *Screening Assessment for the Challenge Guanidine, N,N′-Diphenyl-(Diphenylguanidine)*; Environment Canada and Health Canada; 2013; p 50.

(22) Wastes, Resource Conservation, Common Wastes & Materials, Scrap Tires. *U.S. Environmental Protection Agency*. https://archive.epa.gov/epawaste/conserve/materials/tires/web/html/civil_eng.html (accessed Apr 2, 2021).

(23) McElvery, R. Is the Road to Sustainable Asphalt Paved with Tires? *ACS Cent. Sci.* **2020**, *6* (12), 2120−2122.

(24) Mohajerani, A.; Burnett, L.; Smith, J. V.; Markovski, S.; Rodwell, G.; Rahman, M. T.; Kurmus, H.; Mirzababaei, M.; Arulrajah, A.; Horpibulsuk, S.; Maghool, F. Recycling Waste Rubber Tyres in Construction Materials and Associated Environmental Considerations: A Review. *Resour. Conserv. Recycl.* **2020**, *155*, 104679.

(25) Nanjegowda, V. H.; Biligiri, K. P. Recyclability of Rubber in Asphalt Roadway Systems: A Review of Applied Research and Advancement in Technology. *Resour. Conserv. Recycl.* **2020**, *155*, 104655.

(26) Feraldi, R.; Cashman, S.; Huff, M.; Raahauge, L. Comparative LCA of Treatment Options for US Scrap Tires : Material Recycling and Tire-Derived Fuel Combustion. *Int. J. Life Cycle Assess.* **2013**, *18*, 613−625.

(27) Codling, G.; Yuan, H.; Jones, P. D.; Giesy, J. P.; Hecker, M. Metals and PFAS in Stormwater and Surface Runoff in a Semi-Arid Canadian City Subject to Large Variations in Temperature among Seasons. *Environ. Sci. Pollut. Res.* **2020**, *27* (15), 18232−18241.

(28) Unice, K. M.; Bare, J. L.; Kreider, M. L.; Panko, J. M. Experimental Methodology for Assessing the Environmental Fate of Organic Chemicals in Polymer Matrices Using Column Leaching Studies and OECD 308 Water/Sediment Systems: Application to Tire and Road Wear Particles. *Sci. Total Environ.* **2015**, *533*, 476−487.

(29) Vijayan, A.; Österlund, H.; Marsalek, J.; Viklander, M. Laboratory Melting of Late-Winter Urban Snow Samples: The Magnitude and Dynamics of Releases of Heavy Metals and PAHs. *Water, Air, Soil Pollut.* **2019**, *230* (8), na DOI: 10.1007/s11270-019-4201-2.

(30) Meyer, T.; Wania, F. Organic Contaminant Amplification during Snowmelt. *Water Res.* **2008**, *42* (8−9), 1847−1865.

(31) Johannessen, C.; Helm, P.; Metcalfe, C. D. Detection of Selected Tire Wear Compounds in Urban Receiving Waters. *Environ. Pollut.* **2021**, *287* (June), 117659.

(32) Malmivuo, M.; Luoma, J. Effects of Winter Tyre Type on Roughness and Polishing of Road Surfaces Covered with Ice and Compact Snow. *Eur. Transp. Res. Rev.* **2017**, *9* (1), 1−8.

https://doi.org/10.1021/acs.estlett.1c00682
Environ. Sci. Technol. Lett. 2021, 8, 961−967

(33) Lachance-Tremblay, É.; Perraton, D.; Vaillancourt, M.; Di Benedetto, H. Degradation of Asphalt Mixtures with Glass Aggregates Subjected to Freeze-Thaw Cycles. *Cold Reg. Sci. Technol.* **2017**, *141* (May), 8−15.
(34) Vogelsang, C.; Lusher, A. L.; Dadkhah, M. E.; Sundvor, I.; Umar, M.; Ranneklev, S. B.; Eidsvoll, D.; Meland, S. *Microplastics in Road Dust − Characteristics, Pathways and Measures*; Report sno. 7526-2020; Norwegian Institute for Water Research, 2020.
(35) Sjodin, A.; Ferm, M.; Bjork, A.; Rahmberg, M.; Gudmundsson, A.; Swietlicki, E.; Johansson, C.; Gustafsson, M.; Blomquist, G. *Wear Particles from Road Traffic: A Field, Laboratory, and Modelling Study*; Report number: B1830; IVL Swedish Environmental Research Institute, 2010. DOI: 10.13140/RG.2.2.18594.35524
(36) Furuseth, I. S.; Rødland, E. S. *Reducing the Release of Microplastic from Tire Wear: Nordic Efforts*; Nordic Co-operation, 2020. DOI: 10.6027/NA2020-909
(37) *Design and Development Standards Manual: Section Six - Stormwater Drainage System*; Saskatoon Water Transportation & Utilities Department: City of Saskatoon, 2018.

https://doi.org/10.1021/acs.estlett.1c00682
Environ. Sci. Technol. Lett. 2021, 8, 961−967

SUPPLEMENTARY INFORMATION A

Occurrences of tire rubber derived contaminants in cold-climate urban runoff

Challis, J.K.[1] & Popick, H.[2], Prajapati, S.[3], Harder, P.[4,7], Giesy, J.P.[1,5,6], McPhedran, K.[2], Brinkmann, M.[1,3,7,*]

[1] Toxicology Centre, University of Saskatchewan, Saskatoon, SK, Canada, S7N 5B3

[2] Department of Civil, Geological, and Environmental Engineering, College of Engineering, University of Saskatchewan, Saskatoon, SK, Canada, S7N 5A9

[3] School of Environment and Sustainability, University of Saskatchewan, Saskatoon, SK, Canada, S7N 5C8

[4] Centre for Hydrology, University of Saskatchewan, Saskatoon, SK, Canada, S7N 1K2

[5] Department of Veterinary Biomedical Sciences, University of Saskatchewan, Saskatoon, SK, Canada, S7N 5B4

[6] Department of Environmental Science, Baylor University, Waco, TX, USA, 76706

[7] Global Institute for Water Security, University of Saskatchewan, Saskatoon, SK, Canada, S7N 3H5

*Corresponding author: markus.brinkmann@usask.ca

Contents:

- 27 pages
- 13 Tables
- 12 Figures

1. METHODS

1.1 Reagents

Methanol (LC-MS grade) and dichloromethane (DCM) from Fisher Scientific (Ottawa, ON) and 18.2 MΩ-cm ultrapure water (EMD Milli-Pore Synergy® system, Etobicoke, ON), were used for LC solvents, analytical standards, and sample extractions. All stock solutions were dissolved in 100% methanol (Fisher Scientific). Optima LC/MS grade formic acid was purchased from Fisher Scientific for LC solvent preparation.

1.2 Sampling and Extractions

1.2.1 Stormwater. Grab sampling was used to collect stormwater from seven outfalls during four wet weather events between June and August 2019, listed in Table S1. Equipment used to sample included a 5 L plastic pail secured to a length of rope, 4 L and 1 L Nalgene bottles with caps, and a funnel for transferring sample to the bottles. With the exception of the June 12 event (where only one team was deployed), two sampling teams were deployed at the start of a precipitation event to ensure the timing of sampling was similar at each site. One team sampled MacPherson Ave., 14th St. E, 17th St. W, and 23rd St. E outfalls, while the other sampled Circle Dive Bridge E, Circle Dive Bridge W, and the Silverwood Dog Park outfalls. Teams recorded their time of arrival to each outfall with no set sampling order. This configuration minimized traffic-related uncertainty with routing to each outfall location during potentially heavy storms.

Each sampling event typically took place as soon as precipitation was observed from the USask Environmental Engineering labs, with the exception of the July 25th event (SI-B2). Teams were not able to sample the major storm on July 24, and thus sampling occurred the following day during a relatively small rain event on July 25, approximately 24 hours after the start of the July 24th event. Exact timing of sampling is shown in the precipitation plots in SI-B2. Four of six possible sampling events (i.e., storms occurring during daylight hours) were captured during the 2019 season.

Each sampling site did not have a unique weather station to reference so a number of the sites share the same precipitation data in SI-B2. Each weather station was chosen based on proximity to sampling site. Precipitation data and was taken from Weather Underground (https://www.wunderground.com/weather/ca/saskatoon).

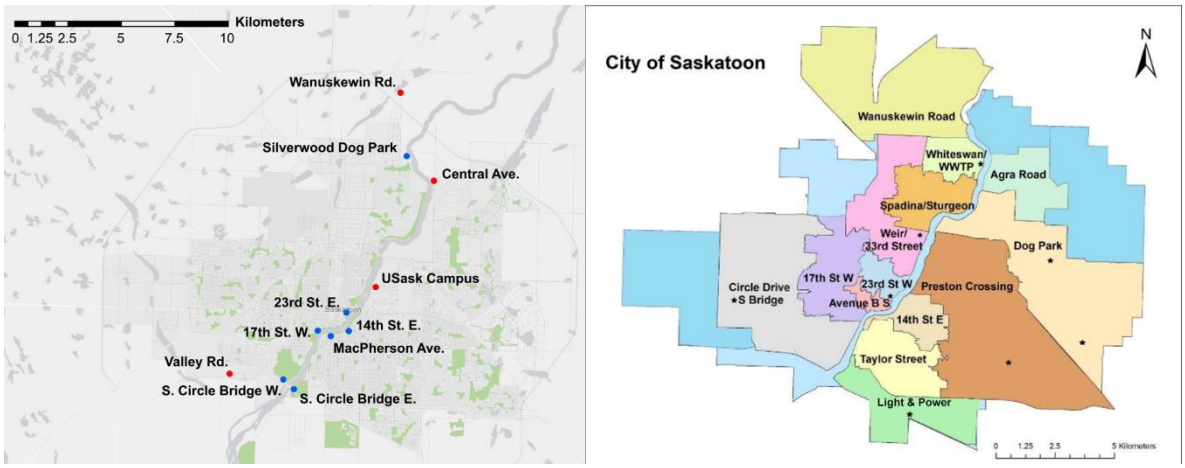

Figure S1: City of Saskatoon stormwater (blue) and snowmelt (red) sampling sites (left) and land-use area map (right). SI-B1 has more details on the land-use areas.

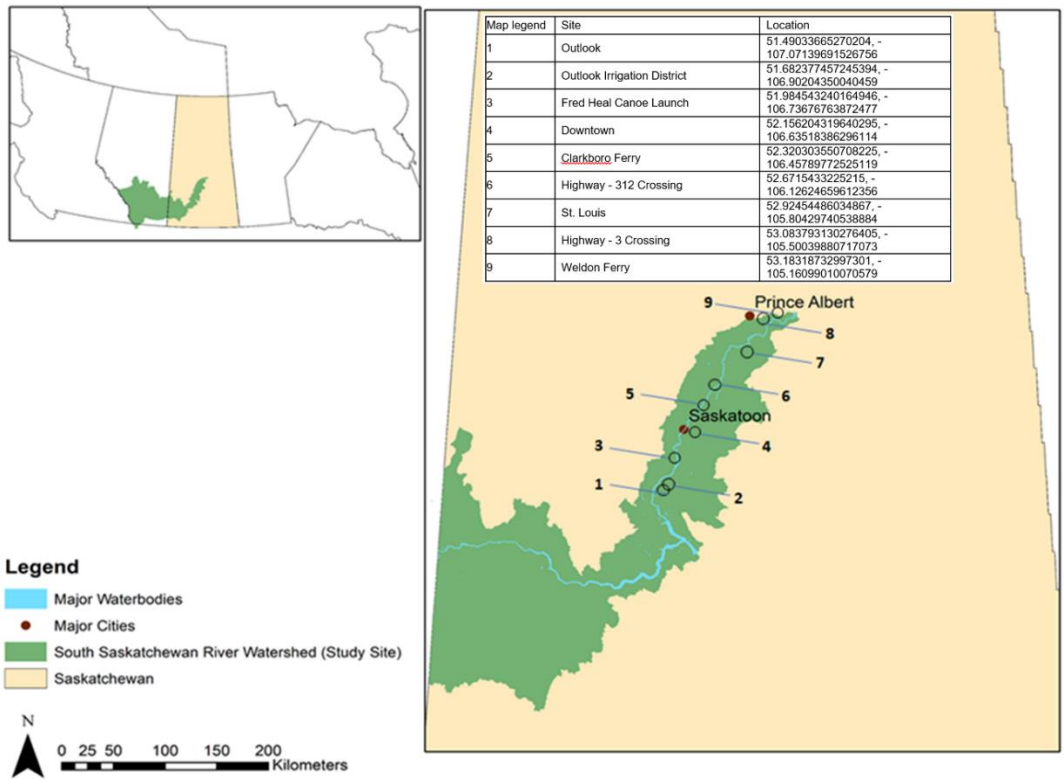

Figure S2: South Saskatchewan River sampling locations.

Table S1. Summer storm events in which stormwater was sampled from outfalls within the City of Saskatoon. Outfalls are identified using the names of proximate locations within the city. Sampling commenced close to storm onset; the July 25 samples were taken the morning after the storm event. All outfalls were sampled during all events for a parallel study; sampling events for which vulcanizer data was analyzed are noted with an asterisk**.** Exact sampling times in relation to each precipitation event can be found in SI-B2.

		Stormwater						
Year	**Date**	**S. Circle Dr. Bridge E.**	**S. Circle Dr. Bridge W.**	**MacPherson Ave.**	**14th St. E.**	**17th St. W.**	**23rd St. E.**	**Silverwood Dog Park**
2019	12-Jun	*	*	*	*	*	*	*
	20-Jun	*	*	*	*	*	*	*
	25-Jul	*	*		*			
	22-Aug		*			*	*	*

Table S2. Snowmelt sampling events from snow storage facilities within the City of Saskatoon. Facilities were selectively sampled; sampling events are noted with an asterisk. Both snow from the pile and snowmelt were collected.

		Snow			
Year	**Date**	**Valley Rd.**	**USask**	**Central Ave.**	**Wanuskewin Rd.**
2019	April 2		***		
	April 13	*	*		*
	April 18	*		*	*
	April 24	*	*	*	*
2020	March 7	***	***		
	March 26	**			
	March 29	**			
	April 10	**			
	April 17	**	**	**	**
	April 20	**			
	April 23	**	**	**	**
	April 28	**	**	**	
	May 1	**	**		**
	May 5	**	**	**	
	May 12	**	**		**

*Snow pile samples collected only
**Snowmelt samples collected only
***Both snow pile and snowmelt samples collected

1.2.2 Snow and snowmelt. There are 4 snow storage facilities within the City of Saskatoon, all of which were included in the present study (Figure S1). These sampling sites include the impermeable site on the southwest border of the City (Valley Rd.), one site north of the City along Wanuskewin Rd., one site located in the northeast of the City (Central Ave.) and one located within the University of Saskatchewan grounds (USask Campus). The Valley Rd. site

has a paved surface, a settling pond, and a designated outlet to the South Saskatchewan River (SSR). Melt water from the Valley Rd. Snow Management Facility runs through an oil and grit separator into a meltwater/stormwater pond. The meltwater then enters a series of specially designed barriers before being discharged. The other 3 sites do not regulate snowmelt flow and lie adjacent to vegetated wetlands or swales that flow into the SSR.

After a snowfall event, snow is plowed to the roadside, later collected in a truck, and transported to one of the snow dumps. Roadside snow from various parts of the city is deposited into one large pile at these sites where it remains exposed to the environment over the winter and spring. Snowmelt was collected from at least one of the four snow facilities on warm days. Snow piles were sampled four times in April 2019 and snowmelt puddles were sampled eleven times from March to May 2020; locations and dates are listed in Table S2. Plastic scoops were used to collect both snow and snowmelt in 4 L or 25 L Nalgene water containers. Snow from the piles was collected from 8-12 random locations on the surfaces and sides of the snow piles to create an aggregate sample of the pile. Snowmelt samples were obtained from meltwater pools found at the foot of snow piles, also collected from various on-site puddles to create an aggregate sample of the snowmelt runoff. Both stormwater and snowmelt samples were sealed, labelled, and transported back to the USask Environmental Engineering labs for storage at 4 °C. Snow pile samples were melted in their Nalgene containers at 21 °C in lab before storage at 4 °C. The purpose of the snow sampling approach was to provide a comparison to the stormwater data in order to understand the degree to which snow contributes to the occurrence of these compounds. This sampling approach did not facilitate the delineation of the dynamics and fate within the snow dump and during melt events.

1.2.3 Lidar data. A Riegl miniVUX1-UAV lidar with an Applanix APX-20 inertial measurement unit (IMU) mounted on a DJI M600 Pro unoccupied aerial system (UAS) platform was used to scan the City of Saskatoon snow dump. The raw IMU trajectory and laser returns were

processed to a georectifed point cloud (110 pts m^{-2}) with the Riegl RiProcess software suite. The difference between the rasterised bare surface, interpolated from the exposed concrete pad around the snow pile, and the rasterised snow surface estimates a snow volume of 151,910 m^3. The ±0.09 m vertical accuracy of the UAS-lidar system (Harder et al., 2020) gives a volumetric uncertainty of ±3,442 m^3. For a pile of compacted snow a conservative estimate of snow density of 600 kg m^{-3} (±50 kg m^{-3}) is assumed based on snow density observations of analogous piled snow (Grünewald et al., 2018). Water equivalent (volume*density) of the snow pile at the time of UAS flight is estimated to be 91,146 m^3 with a propagated error of ±10.6%. The snow dump, displayed in terms of snow depth, is visualised in Figure S11. The snow water volume equivalent in the Valley Road snow dump, estimated from unoccupied aerial system lidar data (Fig. S11) on March 13, 2020, was 91,146 m^3 (±10.6%).

Valley Road was chosen for Lidar measurements because it is the City's most modern snow facility and has a concrete slab that is conducive to the aerial measurements. It also has a well-defined drainage system where water collects, while at the other sites, water simply infiltrates into the ground. The three snow dump sites outside of Valley Road are not as closely managed and there was no size data that the city could provide. From our experience visiting each site, and based on Google satellite imagery of all four snow dump sites, Valley Road is approximately two-times the size of the other three sites, which are similar in size to each other.

1.2.4 Sample extraction and processing. Stormwater, snowmelt, and river samples were filtered through Whatman™ GF/F glass microfibre filters (0.7 µm) and extracted prior to analysis. Each batch of samples were processed with a lab and field blank containing Milli-Q H_2O. The lab blank was filled in the lab immediately prior to processing a batch of samples. Field blanks were sample bottles filled with Milli-Q H_2O and taken into the field during sampling to monitor for contamination not originating from the collected samples. Oasis™ HLB solid-phase extraction cartridges (500 mg, 6cc, Waters Corporation, Milford, MA) were pre-conditioned using 3 mL

DCM, followed by 3 mL methanol, and 3 mL ultrapure water. A volume of 500 mL of each sample was vacuum-extracted through the column at a rate of ≈1 drop/second. After extraction, the column was washed with 3 mL of 5% methanol in water and air-dried with suction for 10 minutes. Columns were eluted twice with 5 mL of methanol and once with 5 mL of DCM. The eluate was mixed and then split into two equal portions with one used for other research and the second being reduced to dryness under nitrogen gas and reconstituted in 0.5 mL of a 1:1 methanol: water (v/v) mixture. Due to very large concentrations of DPG in certain SPE samples, direct injection (no pre-concentration or filtering) was conducted for semi-quantification of all stormwater samples. Extraction recoveries are described in Table S7.

1.3 Instrumental Analysis

1.3.1 Targeted analysis method. The Q-Exactive Orbitrap target method used the following positive mode heated electrospray ionization (HESI) source parameters: sheath gas flow = 35; aux gas flow = 10; sweep gas flow = 1; aux gas heater = 400 ^{o}C; spray voltage = 3.8 kV; S-lens RF = 60; capillary temperature = 350 ^{o}C. A Full MS/parallel reaction monitoring (PRM) method was used with the following scan settings: 120,000/30,000 resolution, AGC target = $1x10^{6}/5x10^{5}$, max injection time = 100 ms/100 ms, full MS scan range of 80-600 m/z and PRM isolation window of 1.0 m/z. Inclusion list ions, collision energies, and retention times are provided in Table S5.

Semi-quantification was done using a targeted external calibration method. Given large concentrations of DPG in stormwater SPE samples, direct injection (no pre-concentration or filtering) was conducted for semi-quantification of all stormwater samples. Due to the lack of isotopically labelled internal standards to correct for recovery and ionization effects at the time of extraction and analysis, concentrations reported should be considered semi-quantitative. Based on experimental extraction and matrix effects data (Table S7 – S9) concentrations of the

target compounds reported here may be underestimated by a factor of two or more (SI-A section 2.2).

1.3.2 Suspect screening analysis method. The Q-Exactive Orbitrap suspect screening method used the following positive mode HESI source parameters: sheath gas flow = 35; aux gas flow = 10; sweep gas flow = 1; aux gas heater = 400 ^{o}C; spray voltage = 3.8 kV; S-lens RF = 60; capillary temperature = 350 ^{o}C. A Full MS-ddMS2 Top 10 method was used with the following Full MS/ddMS2 scan settings: 60,000/15,000 resolution, AGC target = $5x10^5/1x10^5$, max injection time = 100 ms/100 ms, full scan range of 70-1000 m/z, MS2 isolation window = 2.0 m/z, loop count = 5, MSX count = 1, and a stepped NCE = 15, 30, 45.

1.3.3 Batch analyses. Mixed calibration standards (all five target analytes in a mixture) were run at the beginning of each sample batch along with instrument blanks run between every 5-7 samples and single calibration standards (10 or 50 ng mL^{-1}) every 15-20 samples to check for instrument drift. Three separate batch analyses was conducted for 2019 stormwater samples, 2019 snowmelt samples, and 2020 snowmelt samples. The instrument operator setting up the batch analyses did not have knowledge of the site codes and thus samples were placed in an unknown order throughout the batch. Standard check concentrations within 20% of target were deemed acceptable. An eight point calibration curve ranging from 0.1– 2000 ng mL^{-1} was used for semi-quantification. Limits of detection and linearity are shown in Table S6.

1.3.4 Data analysis. Suspect screening was conducted using Compound Discoverer 2.1 (CD) and targeted semi-quantification was done with TraceFinder 4.1 (ThermoFisher Scientific). Suspect screening was conducted using a CD workflow and used mzCloud for suspect identification. All workflow details are provided in Fig. S8 and S9. A conservative, tiered approach for data reduction started by comparing features in blanks versus samples. The first

pass of the data filtered those features with 10-fold greater peak area in samples compared to blanks. A second, more conservative filter looked at those features that were present in samples only (not found in blanks). Additionally, tentative identifications of compounds were based only on those features that had triggered at least one MS2 experiment. Suspect features with match scores in mzCloud ≥80 were considered further. Lab, field, and instrument blanks were used in the suspect screening workflow for identifying features not derived from the environmental samples.

Table S3. Positive mode suspect screening gradient elution method. Flow rate = 0.2 mL/min, column temperature = 40 °C, solvent A = 95% H_2O: 5% MeOH + 0.1% formic acid and B = 100% MeOH + 0.1% formic acid.

Time (min)	%B
0.00	5
7.50	40
15.00	100
20.00	100
20.10	5
25.00	5

Table S4. Positive mode targeted gradient elution method. Flow rate = 0.2 mL/min, column temperature = 40 °C, solvent A = 95% H_2O: 5% MeOH + 0.1% formic acid and B = 100% MeOH + 0.1% formic acid.

Time (min)	%B
0.00	5
4.00	100
5.50	100
5.51	5
7.50	5

Table S5. Precursor and product ions ($[M+H]^+$), collision energy (HCD), and retention time details for the full-scan parallel reaction monitoring Orbitrap™ mass spectrometer method.

Compound Name	Precursor Ion	Product Ion	HCD	Ret Time (min)
6PPD-q	299.1754	215.0819 187.0869 241.0974 256.1210 200.0071 243.1132 100.1122	40	6.29
6PPD-q-d5	304.2068	220.1126 192.1177 246.1281 261.1516 205.1019 248.1440	40	6.30
DPG	212.1184	119.0604 94.0651 195.0917	50	4.48
CPU	219.1492	94.0651 137.0710	45	6.05
DCA	196.2057	83.0854 114.1277	60	5.05
DCU	225.1958	100.1120 143.1179	40	6.12

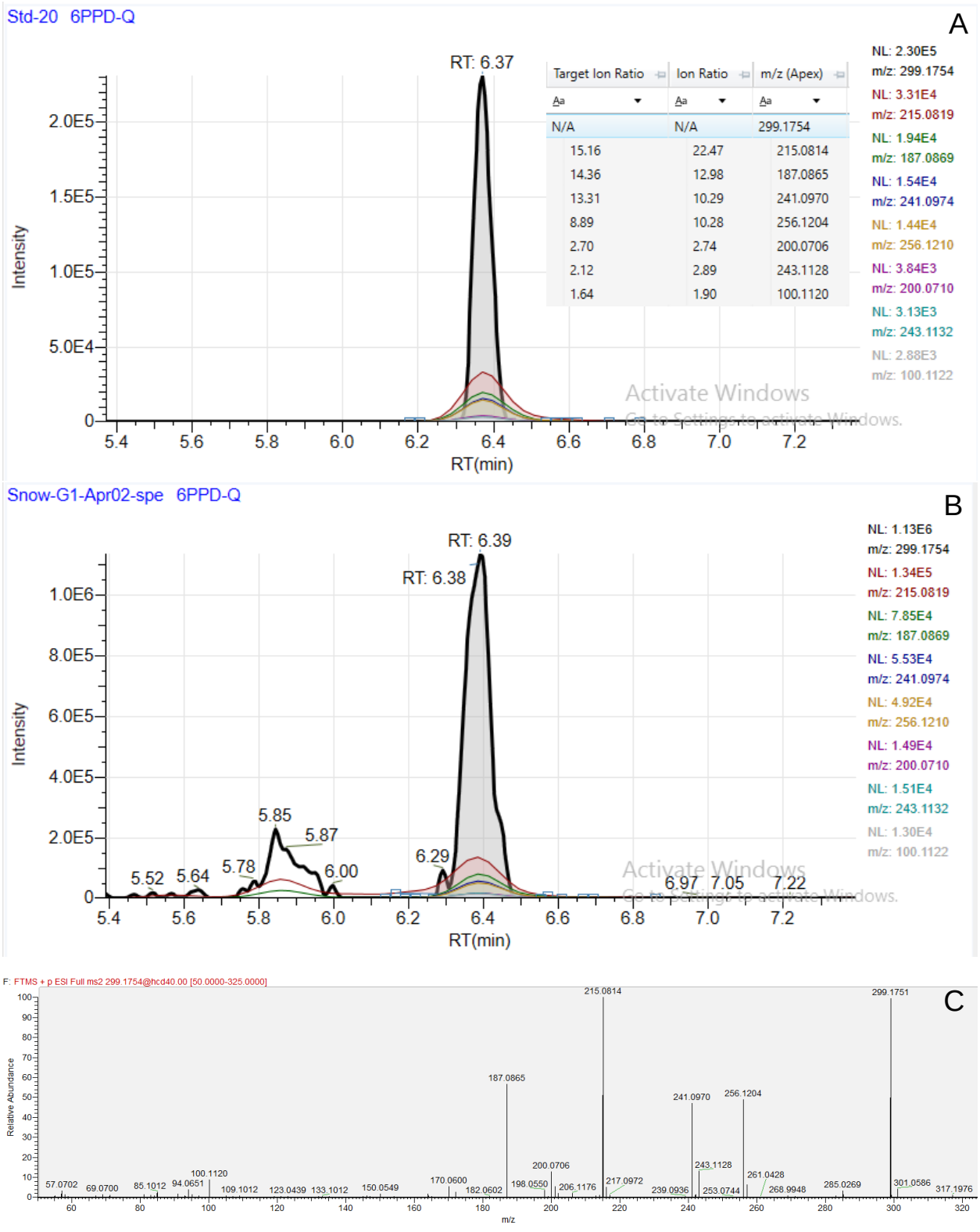

Figure S3: Chromatogram of a 20 µg/L standard (A) and stormwater/snowmelt sample (B) and MS2 spectra (C) of 6PPD-quinone. The black trace in A and B is the parent ion and the coloured traces are the daughter ions corresponding to the legend on the right. The daughter-to-parent ion ratios are provided in the table in (A).

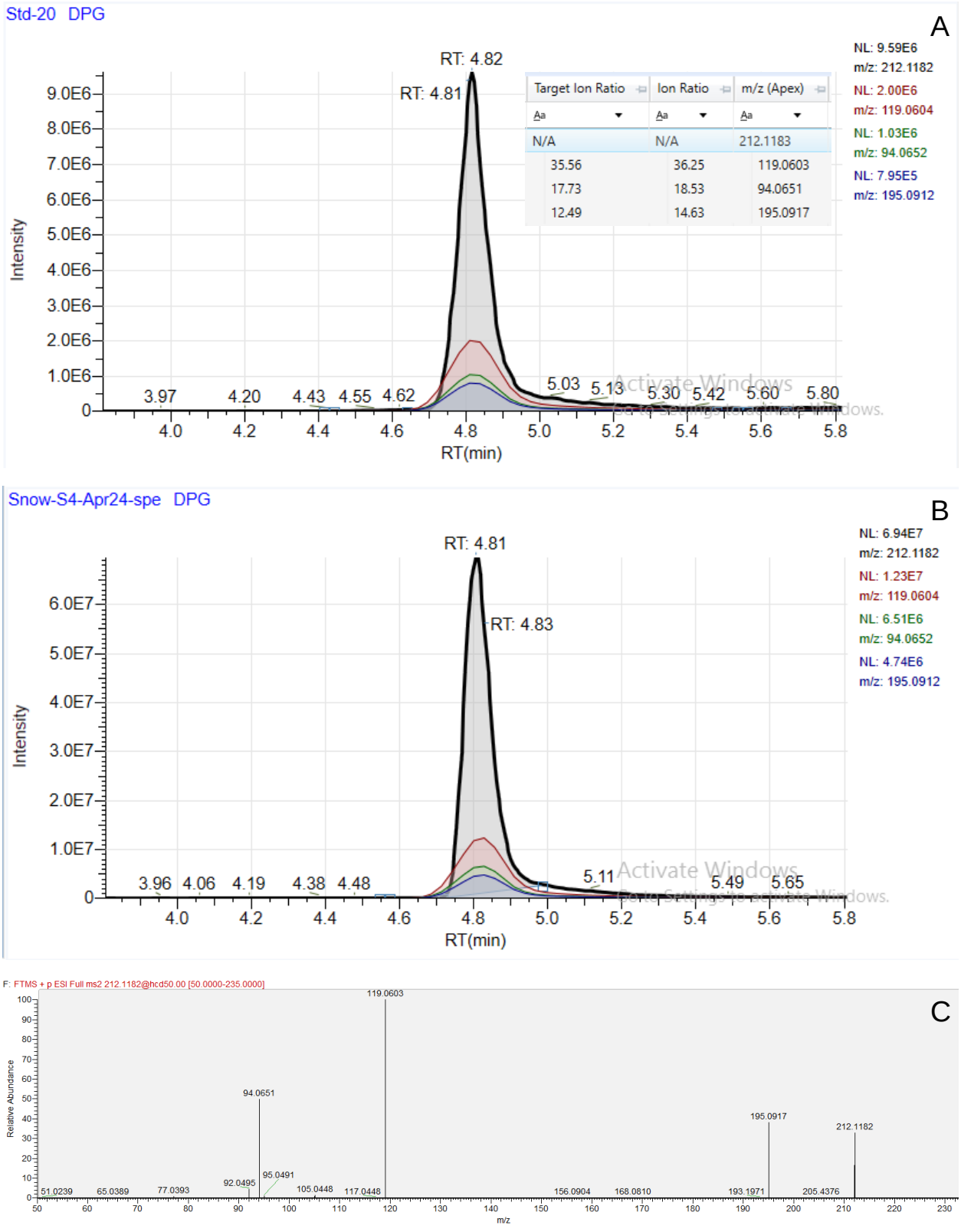

Figure S4: Chromatogram of a 20 µg/L standard (A) and stormwater/snowmelt sample (B) and MS2 spectra (C) of N,N'-diphenylguanidine (DPG). The black trace in A and B is the parent ion and the coloured traces are the daughter ions corresponding to the legend on the right. The daughter-to-parent ion ratios are provided in the table in (A).

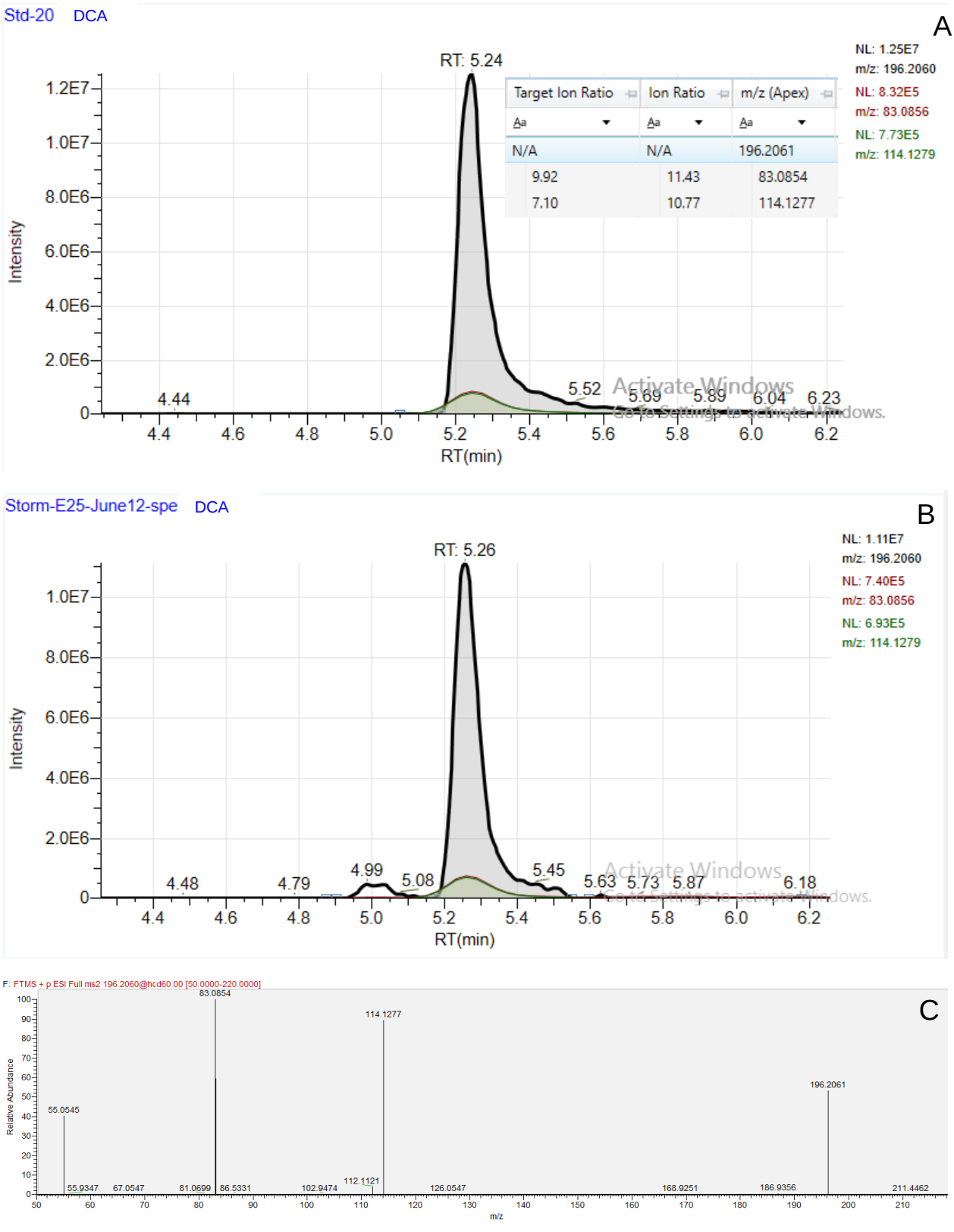

Figure S5: Chromatogram of a 20 µg/L standard (A) and stormwater/snowmelt sample (B) and MS2 spectra (C) of N,N-Dicyclohexylmethylamine (DCA). The black trace in A and B is the parent ion and the coloured traces are the daughter ions corresponding to the legend on the right. The daughter-to-parent ion ratios are provided in the table in (A).

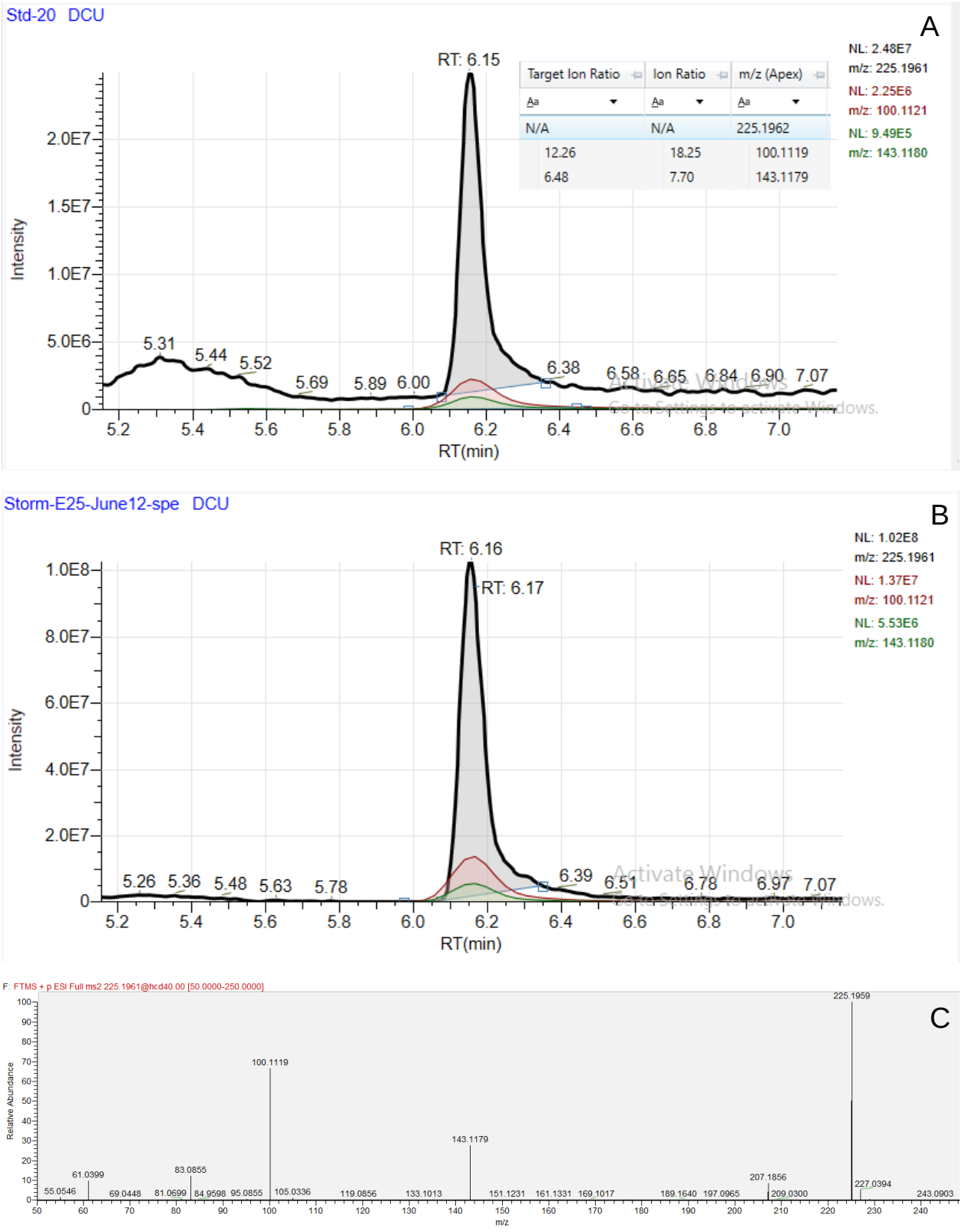

Figure S6: Chromatogram of a 20 µg/L standard (A) and stormwater/snowmelt sample (B) and MS2 spectra (C) of N,N'-Dicyclohexylurea (DCU). The black trace in A and B is the parent ion and the coloured traces are the daughter ions corresponding to the legend on the right. The daughter-to-parent ion ratios are provided in the table in (A).

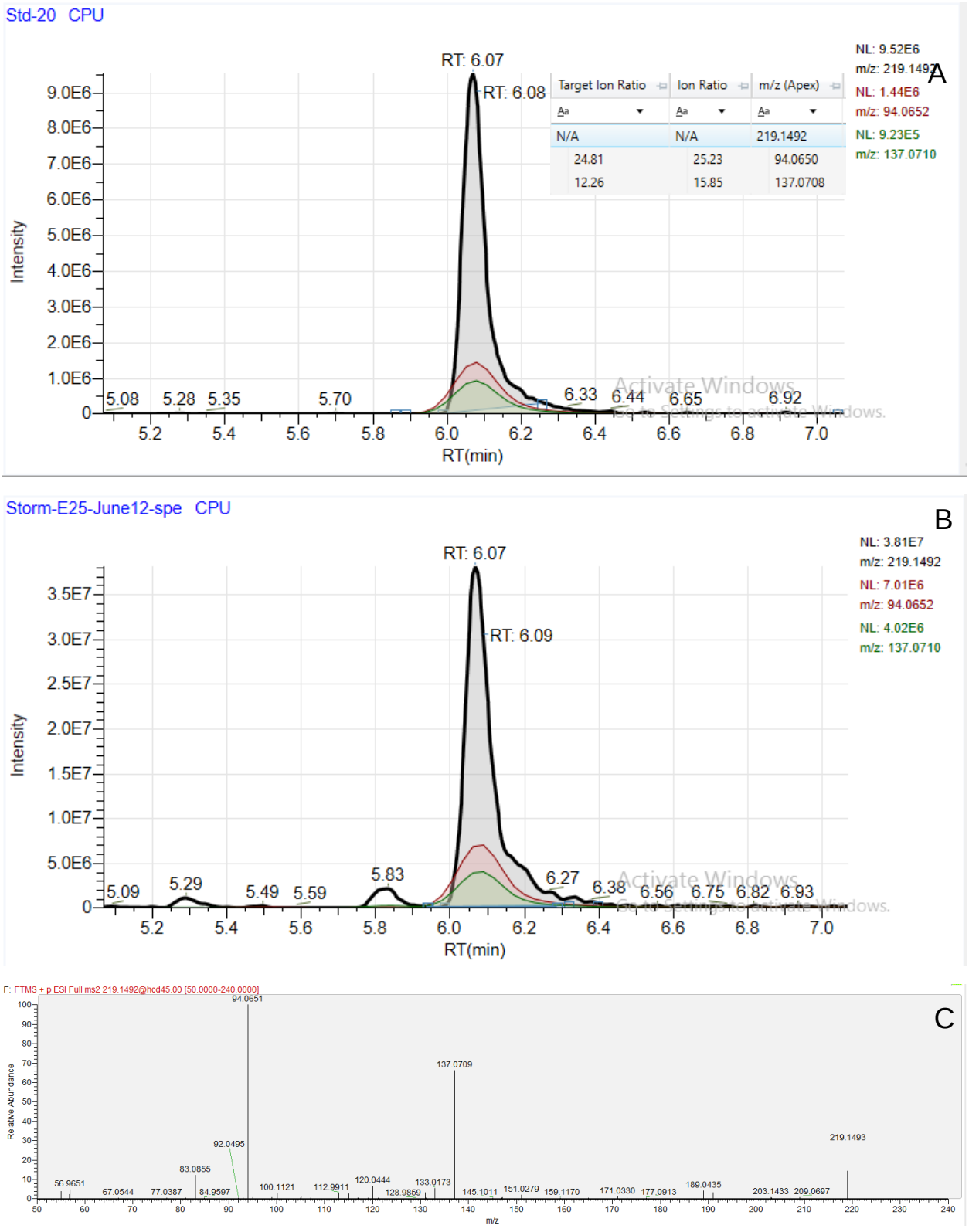

Figure S7: Chromatogram of a 20 µg/L standard (A) and stormwater/snowmelt sample (B) and MS2 spectra (C) of 1-Cyclohexyl-3-phenylurea (CPU). The black trace in A and B is the parent ion and the coloured traces are the daughter ions corresponding to the legend on the right. The daughter-to-parent ion ratios are provided in the table in (A).

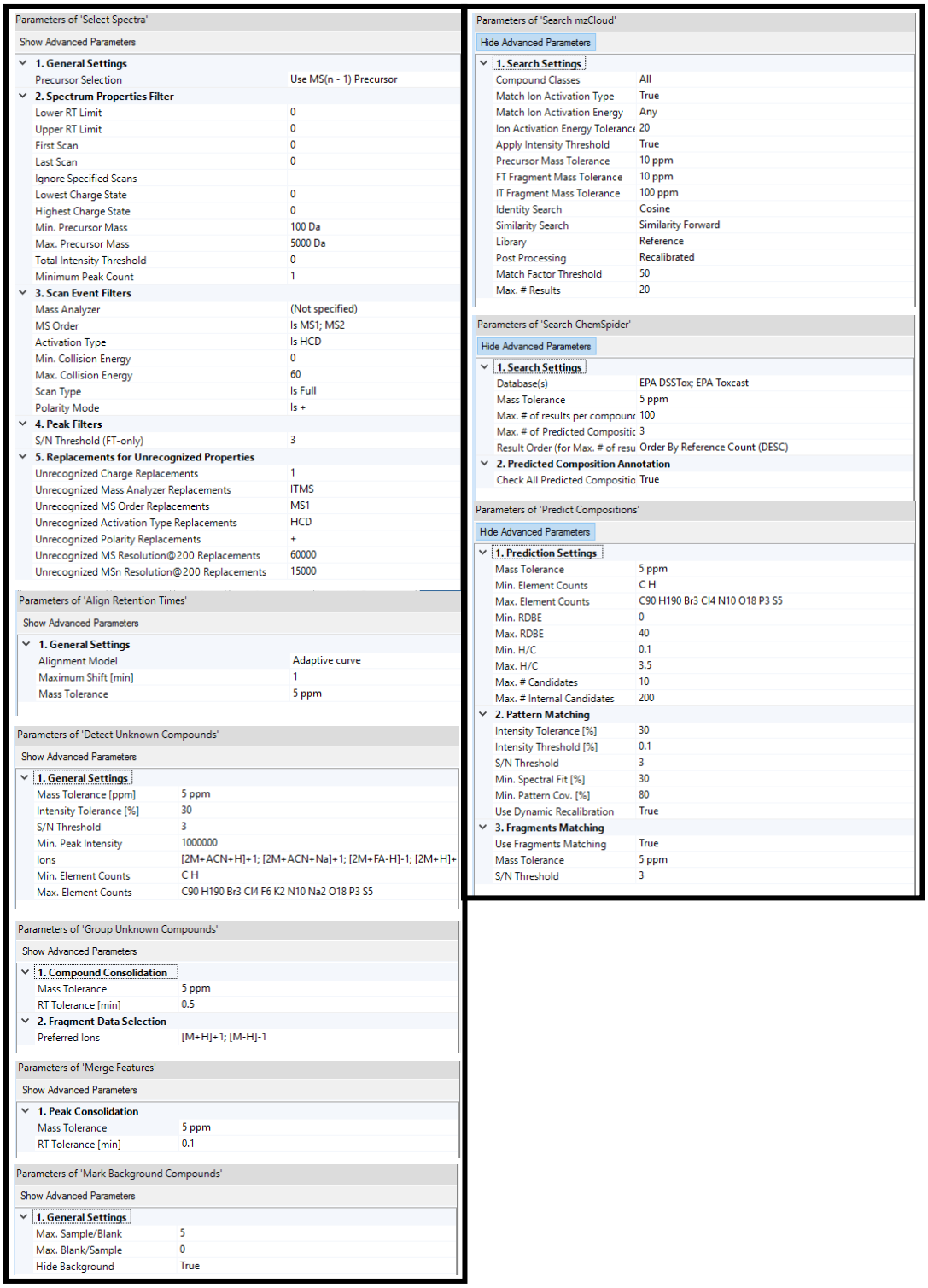

Figure S8: Compound Discoverer v2.1 data workflow settings.

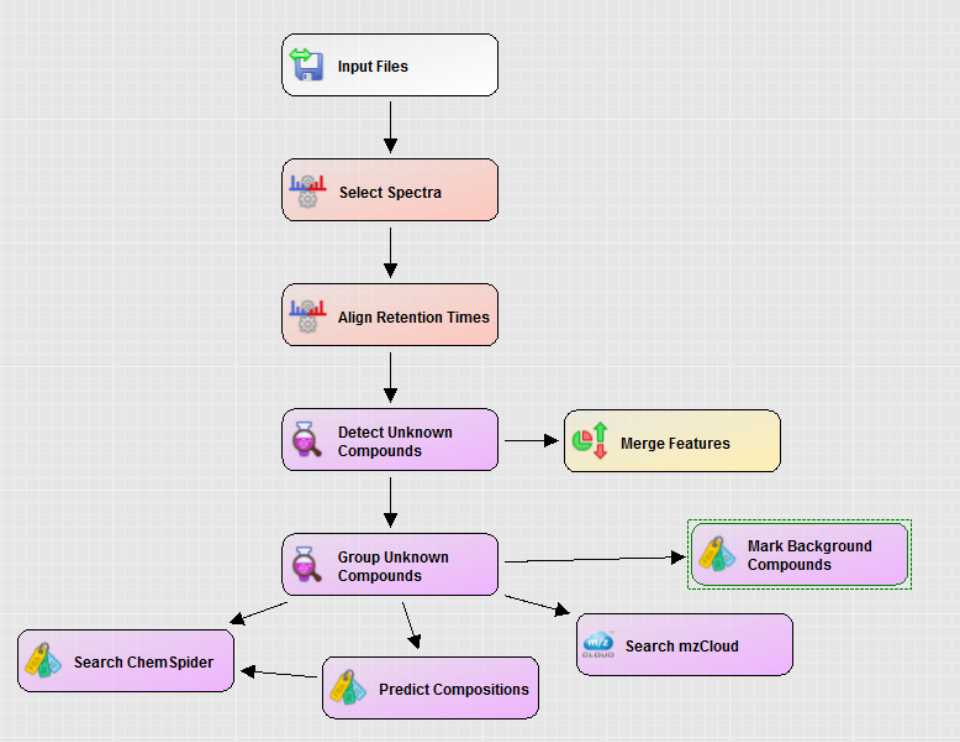

Figure S9: Compound Discoverer v2.1 data workflow.

2. RESULTS

2.1 Detection Limits

Method detection (Table S6) limits were determined using a procedural extraction blank, extracted and processed as detailed above in section 1.2.4. Each procedural blank sample was measured in seven consecutive injections. Slopes from the calibration curve run in the same batch of samples were used in the LOD and LOQ calculations. Limit of detection (LOD) and limit of quantitation (LOQ) calculated as $(X_{BLK} + 3\sigma_{BLK})$/slope and $(X_{BLK} + 10\sigma_{BLK})$/slope, respectively.

Table S6: Detection limits and calibration curve linearity for the target compounds.

Compound	LOD (ng mL^{-1})	LOQ (ng mL^{-1})	Linearity[a]
6PPD-quinone	1.2	3.3	>0.9986
DPG	0.4	1.1	>0.9988
DCA	0.3	0.8	>0.9946
DCU	0.5	1.2	>0.9993
CPU	0.4	1.2	>0.9995

6PPD-quinone = 2-anilo-5-[(4-methylpentan-2-yl)amino]cyclohexa-2,5-diene-1,4-dione; DPG = N,N'-Diphenylguanidine; DCA = N,N-Dicyclohexylmethylamine; DCU = N,N'-Dicyclohexylurea; CPU = 1-Cyclohexyl-3phenylurea.
a – the lowest r^2 value of four calibration curves from separate analyses

2.2 Sample recoveries and matrix effects. Spike and recoveries were conducted in lab and river water using the method described in main text. Recoveries represent losses incurred during sample processing (e.g., filtering, SPE, nitrogen evaporation) and ion suppression in the HESI source due to matrix effects. Total recoveries from river water ranged from 66 – 88% (Table S7), with the exception of DCA (21% recovery). Because these target compounds were first identified via suspect screening and re-analyzed with standards retrospectively, the extraction method could not be optimized for DCA. Recovery factors were not applied to the data, therefore reported concentrations of DCA are potentially underestimated by up to 80% and should be treated qualitatively compared to the other reported compounds.

Table S7: Total recoveries of the target compounds spiked at 50 µg/L in lab water (Milli-Q) and river water and extracted using SPE.

Compound	Lab water (µg/L)			River water (µg/L)		
	AVE[a]	SD	% Recovery[b]	AVE[a]	SD	% Recovery[b]
6PPD-quinone	35.0	3.1	70	44.1	1.8	88
DPG	46.2	2.2	92	33.1	2.6	66
DCA	33.3	1.4	67	10.4	1.2	21
DCU	50.9	1.4	102	39.9	1.7	80
CPU	47.5	1.5	95	34.1	1.2	68

6PPD-quinone = 2-anilo-5-[(4-methylpentan-2-yl)amino]cyclohexa-2,5-diene-1,4-dione; DPG = N,N-Diphenylguanidine; DCA = N,N-Dicyclohexylmethylamine; DCU = N,N'-Dicyclohexylurea; CPU = 1-Cyclohexyl-3-phenylurea.
a – average (AVE) and standard deviation (SD) of triplicate samples.
b - % recovery = (average concentration / 50 µg/L) x 100%.

In addition to the spike and recovery experiments, because all samples were measured by SPE and direct injection (to ensure the high DPG concentration samples fell within the linear dynamic range of 0.5 – 2000 ng/mL) they could be compared to assess recoveries in storm and snow sample matrices (Table S8). Direct injection samples and those SPE samples with DPG concentrations <2000 ng/mL were compared (n=17). SPE samples were on average 76±20% of the direct injection concentrations, suggesting average loss of 24% during the SPE extraction process. This agrees well with method recoveries assessed in lab (92%) and river water (66%) (Table S7).

Matrix effects were retrospectively assessed using the isotopically labelled internal standard 6PPD-quinone-d5, which was acquired well after all samples were extracted and analyzed. This was done by spiking six random stormwater SPE samples and six Milli-Q H_2O blank samples with 6PPD-quinone-d5 at 50 ng mL^{-1}. Peak areas in stormwater matrix were on average ≈50% of the peak areas in the Milli-Q H_2O matrix. The matrix spikes were only conducted in replicate for 6PPD-quinone-d5 (Table S9). In the absence of isotopically labelled standards for DPG, DCA, DCU, and CPU assessment of matrix effects was more difficult given the presence of the native compounds in most samples. The 23rd St. E June 12th sample was the only sample with no detections of any target compounds, based on initial analyses. This sample matrix was used to spike native DPG, DCA, DCU, and CPU at 50 ng mL^{-1} and assess matrix effects compared to similarly spiked Milli-Q H_2O matrix. Peak areas in the stormwater

matrix were less the blank matrix by 44% DPG, 54% DCA, 39% DCU, and 61% CPU. These results suggest that in the absence of isotopically labelled standards, as was the case here, semi-quantification of the target compounds may be underestimating concentrations by at least a factor of 2 when considering recovery losses and matrix effects.

Table S8: Concentrations of DPG in direction injection and SPE stormwater and snowmelt samples.

Direct injection (ng mL^{-1})	**SPE (ng mL^{-1})**	**% Ratio (SPE/Direct)**
0.79	0.87	110%
2.07	1.68	81%
0.84	0.65	78%
0.49	0.55	112%
1.04	0.90	87%
0.69	0.45	66%
1.24	0.74	60%
1.18	0.87	74%
0.39	0.15	39%
1.22	0.63	52%
2.96	1.53	52%
1.19	0.98	82%
0.54	0.39	72%
1.45	1.43	99%
1.81	1.24	68%
Average		**76%**
Standard deviation		**20%**

Table S9: Peak areas of 6PPD-quinone-d5 internal standard spiked at 50 ng mL^{-1} in six blank samples (Milli-Q H_2O) and six stormwater SPE samples.

Sample number	**Blank spike peak area**	**Sample spike peak area**
1	1.16×10^8	9.02×10^7
2	1.17×10^8	8.06×10^7
3	1.21×10^8	6.95×10^7
4	1.18×10^8	2.67×10^7
5	1.23×10^8	1.71×10^7
6	1.30×10^8	4.10×10^7
Average	**1.15×10^8**	**5.42×10^7**
Standard deviation	**1.06×10^7**	**3.01×10^7**
Average % ratio (sample/blank)	**47%**	

2.3 Sample Concentrations

Table S10: Concentrations (ng L^{-1}) of tire rubber-derived compounds in snowmelt samples from 2019 and 2020. Each cell shows the average concentration (top number), standard deviation (middle number), and detection frequency (bottom number, detections/sampling events) over all sampling events at a single site. The bottom row of the table provides summary statistics for each compound across all sites and sampling events.

Sampling site	6PPD-q (ng L^{-1})		DPG (ng L^{-1})		DCA (ng L^{-1})		DCU (ng L^{-1})		CPU (ng L^{-1})	
	2019	2020	2019	2020	2019	2020	2019	2020	2019	2020
USask Campus	536 ± 179 (4/4)	59 ± 54 (7/7)	1,178 ± 494 (4/4)	754 ± 483 (7/7)	10 ± 8.4 (4/4)	4.3 ± 2.8 (4/7)	136 ± 47 (2/4)	33 ± 22 (4/7)	125 ± 87 (4/4)	5.6 ± 1.4 (3/7)
Central Ave	250 (1/1)	83 ± 65 (2/3)	493 (1/1)	552 ± 124 (2/3)	3.5 (1/1)	4.1 ± 1.8 (2/3)	<1.2	63 ± 87 (2/3)	46 ± (1/1)	27 ± 34 (3/3)
Wanuskewin Rd	152 ± 81 (3/3)	63 ± 43 (3/3)	452 ± 294 (3/3)	828 ± 1027 (3/3)	6.2 ± 2.1 (3/3)	3.7 ± 0.3 (2/3)	<1.2	35 ± 11 (2/3)	29 ± 24 (3/3)	4.9 ± 3.5 (3/3)
Valley Rd	409 ± 17 (2/2)	110 ± 48 (7/9)	561 ± 239 (2/2)	1,607 ± 2,699 (9/9)	6.4 ± 0.4 (2/2)	3.2 ± 0.6 (5/9)	<1.2	22 ± 10 (2/9)	44 ± 14 (2/2)	4.8 ± 2.7 (7/9)
AVE	**367**	**81**	**768**	**1,111**	**7.7**	**3.8**	**136**	**37**	**72**	**9.2**
SD	**206**	**53**	**483**	**1,814**	**5.6**	**1.6**	**47**	**35**	**69**	**15**
MIN	**74**	**15**	**113**	**119**	**3.5**	**2.0**	**102**	**1.6**	**16**	**2.3**
MAX	**756**	**172**	**1,851**	**8,667**	**23**	**8.4**	**169**	**125**	**217**	**65**
% Detection	**100**	**86**	**100**	**95**	**100**	**59**	**20**	**45**	**100**	**73**

6PPD-quinone = 2-anilo-5-[(4-methylpentan-2-yl)amino]cyclohexa-2,5-diene-1,4-dione; DPG = N,N'-Diphenylguanidine; DCA = N,N-Dicyclohexylmethylamine; DCU = N,N'-Dicyclohexylurea; CPU = 1-Cyclohexyl-3-phenylurea; ND = non-detect.

Sampling dates: USask 2019 = April 2, 13, 18, 24; USask 2020 = March 7, April 17, 23, 28, May 5, 12; Central 2019 = April 24; Central 2020 = April 23, 28, May 5; Wanuskewin Rd 2019 = April 13, 18, 24; Wanuskewin Rd 2020 = April 17, 28, May 12; Valley 2019 = April 13, 18; Valley 2020 = March 26, 29, April 10, 17, 20, 23, 28, May 1, 12.

Table S11: Concentrations (ng L^{-1}) of tire-rubber related compounds in stormwater samples from 2019. Each cell shows the average concentration (top number), standard deviation (middle number), and detection frequency (bottom number, detections/sampling events) over all sampling events at a single site. The bottom row of the table provides summary statistics for each compound across all sites and sampling events.

Sampling site	6PPD-q (ng L^{-1})	DPG (ng L^{-1})	DCA (ng L^{-1})	DCU (ng L^{-1})	CPU (ng L^{-1})
	2019	2019	2019	2019	2019
Circle Bridge E	170 ± 94 (2/3)	1,210 ± 1,680 (4/4)*	8.0 ± 9.4 (3/3)	270 ± 219 (3/3)	59 ± 94 (2/3)
Circle Bridge W	746 ± 927 (2/4)	15,800 ± 30,200 (4/4)	13 ± 13 (4/4)	460 ± 620 (4/4)	101 ± 108 (3/4)
MacPherson Ave	212 (1/2)	81,300 ± 139,000 (3/3)*	13 (1/2)	174 ± 48 (2/2)	89 (1/2)
14th St E	863 ± 561 (2/3)	109,000 ± 128,000 (4/4)*	60 ± 0.9 (2/3)	1,890 ± 1,900 (2/3)	198 ± 188 (3/3)
17th St W	487 ± 566 (2/3)	2,300 ± 1,760 (3/3)	37 ± 7.2 (3/3)	261 ± 144 (3/3)	168 ± 134 (3/3)
23rd St E	606 ± 694 (2/3)	124,000 ± 208,000 (3/4)*	58 ± 25 (2/3)	288 ± 169 (2/3)	171 ± 157 (2/3)
Silverwood	1160 (1/3)	91,100 ± 182,000 (4/4)*	29 ± 0.2 (2/3)	148 ± 122 (3/3)	87 ± 74 (3/3)
AVE	593	59,700	29	452	130
SD	525	118,000	22	737	114
MIN	86	10	1.0	6.7	1.9
MAX	1,400	364,000	76	3,230	395
% Detection	57	96	81	90	81

6PPD-quinone = 2-anilo-5-[(4-methylpentan-2-yl)amino]cyclohexa-2,5-diene-1,4-dione; DPG = N,N'-Diphenylguanidine; DCA = N,N-Dicyclohexylmethylamine; DCU = N,N'-Dicyclohexylurea; CPU = 1-Cyclohexyl-3-phenylurea

Sampling dates: Circle Bridge E = June 12, 20, July 25; Circle Bridge W = June 12, 20, July 25, August 22; MacPherson Ave = June 12, 20; 14th St E = June 12, 20, July 25; 17th St W = June 12, 20, August 22; 23rd St E = June 12, 20, August 22; Silverwood = June 12, 20, August 22.

*Additional sample points for DPG due to direct injection analysis of high concentration storm water samples that were not available in sufficient volumes to allow for SPE analysis of the other compounds.

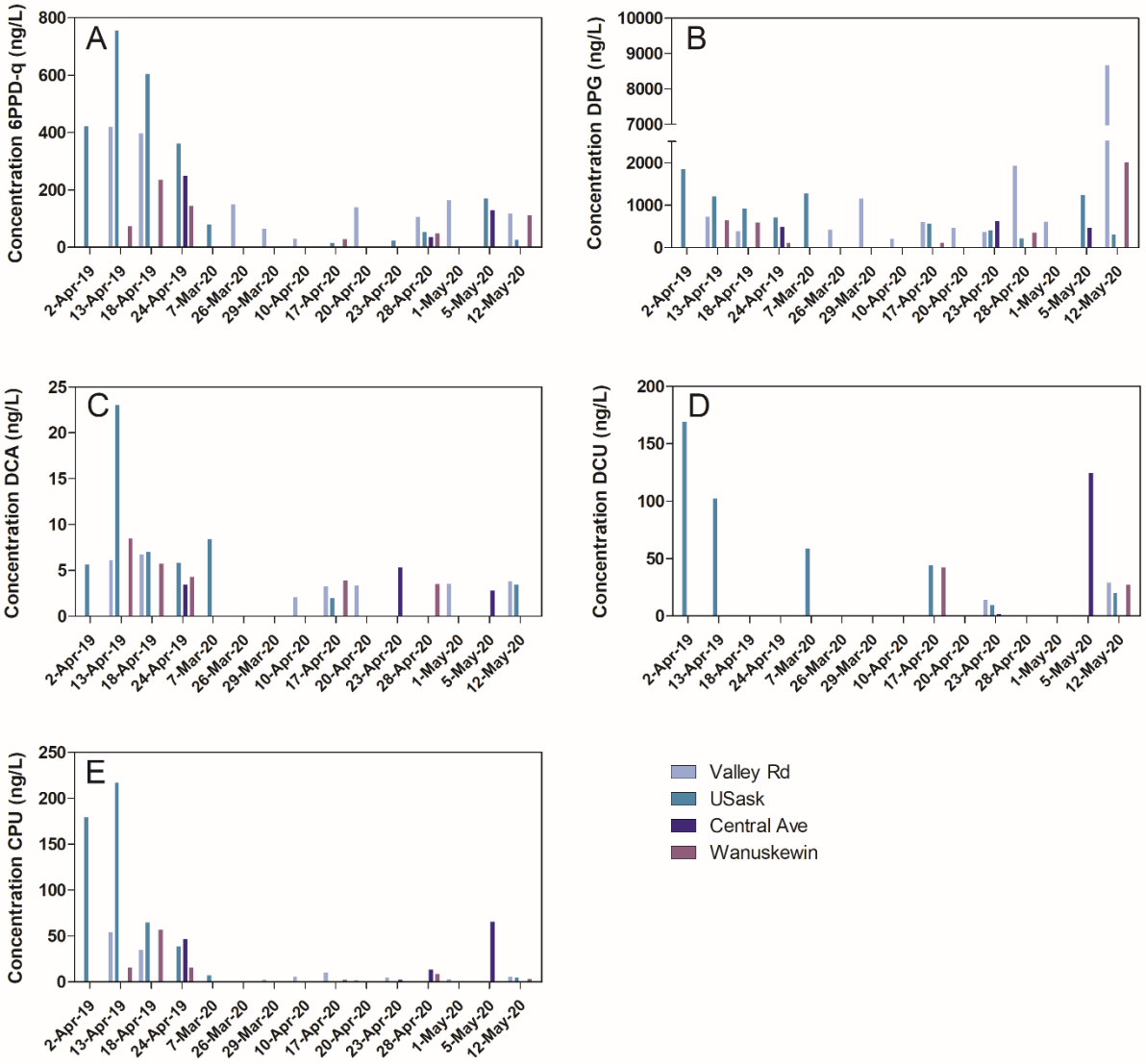

Figure S10: Concentrations (ng L^{-1}) of 6PPD-quinone (A), N,N'-Diphenylguanidine (DPG) (B), N,N-Dicyclohexylmethylamine (DCA) (C), N,N'-Dicyclohexylurea (DCU) (D), and 1-Cyclohexyl-3-phenylurea (CPU) (E) in snow samples from 2019 and snowmelt from 2020. Each bar represents a single sample. Sampling locations correspond to street names in closest proximity to snow dumps. Note the difference in concentration range (ng L^{-1}) in A – E.

2.4 Lidar Snow Data

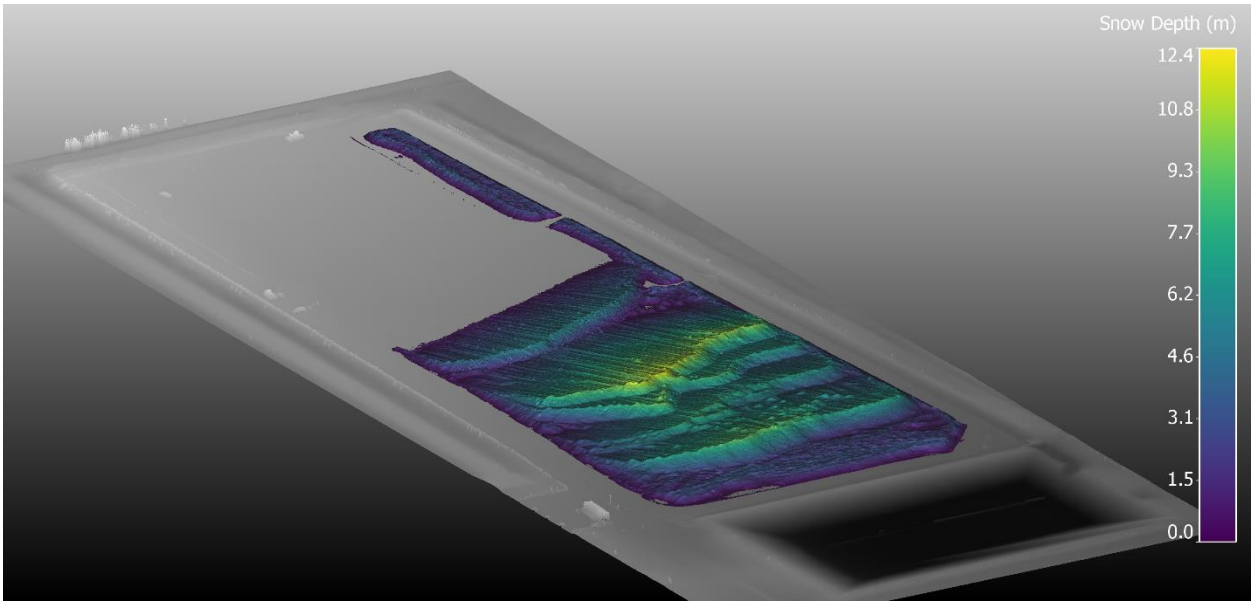

Figure S11: Snow depth (m) of the Valley Road snow dump site from UAS-lidar flight on March 13, 2020 used to estimate the volume of snow and water equivalent for loading calculations.

2.5 Mass Loadings

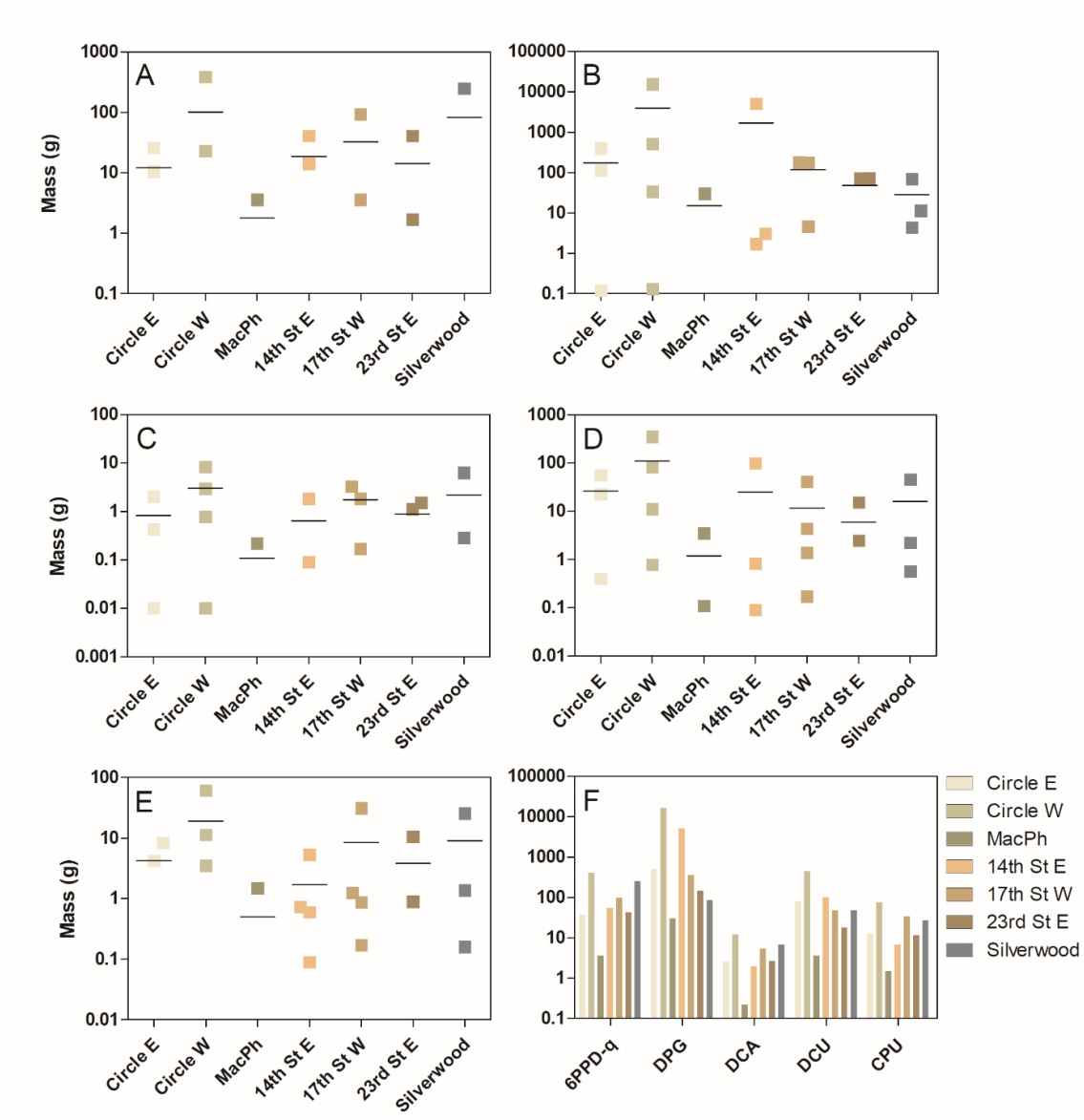

Figure S12: Mass loadings (g) of 6PPD-quinone (A), N,N'-diphenylguanidine (DPG) (B), N,N-dicyclohexylmethylamine (DCA) (C), N,N'-Dicyclohexylurea (DCU) (D), and 1-Cyclohexyl-3-phenylurea (CPU) (E) in stormwater samples from 2019. Individual data points (line = mean) represent loadings calculated using Eq. 1, based on measured concentrations on a given sampling date (June 12, 20, July 25, August 22). Total mass loadings in (F) are the summed loadings at each sampling site over the four runoff events.

2.6 River Concentrations

Table S12: Concentrations (ng L^{-1}) of DPG in the South Saskatchewan River in 2020. The bottom row of the table provides summary statistics across all sites and sampling events. The other four target compounds were not detected in these samples.

Sampling site	Date	DPG (ng L^{-1})
Outlook	9-Jun-20	401
	10-Aug-20	47
	6-Oct-20	5.3
Outlook irrigation district	16-Jun-20	3.3
	10-Aug-20	8.5
	6-Oct-20	0.7
Fred Heal	2-Jun-20	3.6
	10-Aug-20	4.2
	6-Oct-20	3.5
Downtown	2-Jun-20	5.3
	19-Aug-20	8.0
	7-Oct-20	4.1
Clarkboro Ferry	2-Jun-20	1.6
	19-Aug-20	8.2
	7-Oct-20	5.4
Highway 312	3-Jun-20	4.0
	20-Aug-20	15
	7-Oct-20	5.0
St. Louis	3-Jun-20	2.0
	19-Aug-20	22.0
	7-Oct-20	3.7
Highway 3	20-Aug-20	4.6
	8-Oct-20	3.8
Weldon Ferry	18-Jun-20	9.8
	20-Aug-20	29.4
	8-Oct-20	3.3
AVE		**24**
SD		**76**
MIN		**0.7**
MAX		**401**
% Detection		**100**

2.7 Land-Use Correlations

Table S13: Pearson coefficients of determination (r^2 values) for mean mass loadings as a function of land-use class at each sampling site.

Land use class	6PPD-quinone	DPG	DCA	DCU	CPU	Average
Roads	0.878	0.576	0.908	0.753	0.884	0.800
Residential	0.916	0.734	0.954	0.844	0.965	0.883
Commercial	0.666	0.370	0.842	0.519	0.837	0.647
Industrial	0.389	0.004	0.265	0.028	0.122	0.162
Green	0.347	0.000	0.220	0.011	0.088	0.133

3. REFERENCES

Grünewald, T.; Wolfsperger, F.; Lehning, M. Snow farming: conserving snow over the summer season. *The Cryosphere*. **2018**, *12*, 385–400, https://doi.org/10.5194/tc-12-385-2018.

Harder, P.; Pomeroy, J. W.; Helgason, W. D. Improving sub-canopy snow depth mapping with unmanned aerial vehicles: lidar versus structure-from-motion techniques. *The Cryosphere.* **2020**. *14*, 1919–1935, https://doi.org/10.5194/tc-14-1919-2020.

Supplementary information B1: Land use ar

Catchment Name	Area (km2)	Relative Area (%)	Primary Type
Wanuskewin Road	25.50	11.18	Light Industrial
Circle Dr S Bridge	24.60	10.78	Residential
Light & Power	9.58	4.2	Light Industrial
17th St. W.	9.27	4.06	Residential
14 St. E.	3.18	1.39	Residential
MacPherson Ave.	1.47	0.64	Residential
23rd St. W.	2.73	1.2	Commercial & Industrial
Total	76.33707733	33.45	

Catchment	Land Use	CR	% of area
Wanuskewin Rd.	R	0.95	4
(Silverwood Dog Park outfall)	HW	0.95	4
	IN	0.6	37
	GR	0.1	55
Circle Dr. S. Bridge	SR	0.3	35
(S. Circle Dr. Bridge W outfall)	MR	0.6	10
	R	0.95	9
	HW	0.95	7
	CM	0.6	7
	IN	0.6	15
	GR	0.1	17
Light & Power	SR	0.3	25
(S. Circle Dr. Bridge E outfall)	MR	0.6	5
	R	0.95	8
	HW	0.95	8
	CM	0.6	9
	IN	0.6	25
	GR	0.1	20
17th St. W.	SR	0.3	39
	MR	0.6	16
	R	0.95	8
	HW	0.95	5
	CM	0.6	14
	IN	0.6	5
	GR	0.1	5
	AG	0.05	5
14th St. E.*	SR	0.3	54
(outfall within 14th St. E. catchment)	MR	0.6	12
	R	0.95	9
	HW	0.95	4

	CM	0.6	10
	GR	0.1	8
	AG	0.05	3
MacPherson Ave.*	SR	0.3	54
(outfall within 14th St. E. catchment)	MR	0.6	12
	R	0.95	9
	HW	0.95	4
	CM	0.6	10
	GR	0.1	8
	AG	0.05	3
23rd St. W.	SR	0.3	20
	MR	0.6	6
	R	0.95	10
	HW	0.95	6
	CM	0.6	29
	IN	0.6	25
	GR	0.1	4

ea and runoff coefficients of storr

Land use class	Acronym	CR
Single-family Residential	SR	0.3
Multi-family Residential	MR	0.6
Roads	R	0.95
Highways	HW	0.95
Commercial	CM	0.6
Industrial	IN	0.6
Green	GR	0.1
Agricultural	AG	0.05

Fraction of area	Land Use-Specific Area (km2)
0.04	1.02
0.04	1.02
0.37	9.43
0.55	14.02
0.35	8.61
0.1	2.46
0.09	2.21
0.07	1.72
0.07	1.72
0.15	3.69
0.17	4.18
0.25	2.40
0.05	0.48
0.08	0.77
0.08	0.77
0.09	0.86
0.25	2.40
0.2	1.92
0.39	3.61
0.16	1.48
0.08	0.74
0.05	0.46
0.14	1.30
0.05	0.46
0.05	0.46
0.05	0.46
0.54	1.72
0.12	0.38
0.09	0.29
0.04	0.13

0.1	0.32
0.08	0.25
0.03	0.10
0.54	0.79
0.12	0.18
0.09	0.13
0.04	0.06
0.1	0.15
0.08	0.12
0.03	0.04
0.2	0.55
0.06	0.16
0.1	0.27
0.06	0.16
0.29	0.79
0.25	0.68
0.04	0.11

nwater sampling sites

Description
Single dwelling house
Multiple separate housing units within building
With average traffic less than 15,000 vehicles/day
With average traffic more than 15,000 vehicles/day
Downtown, central business district, shopping centre, university, hopsital, etc.
Industrial area
Parks, forests, meadows, and undeveloped area
Cultivated area

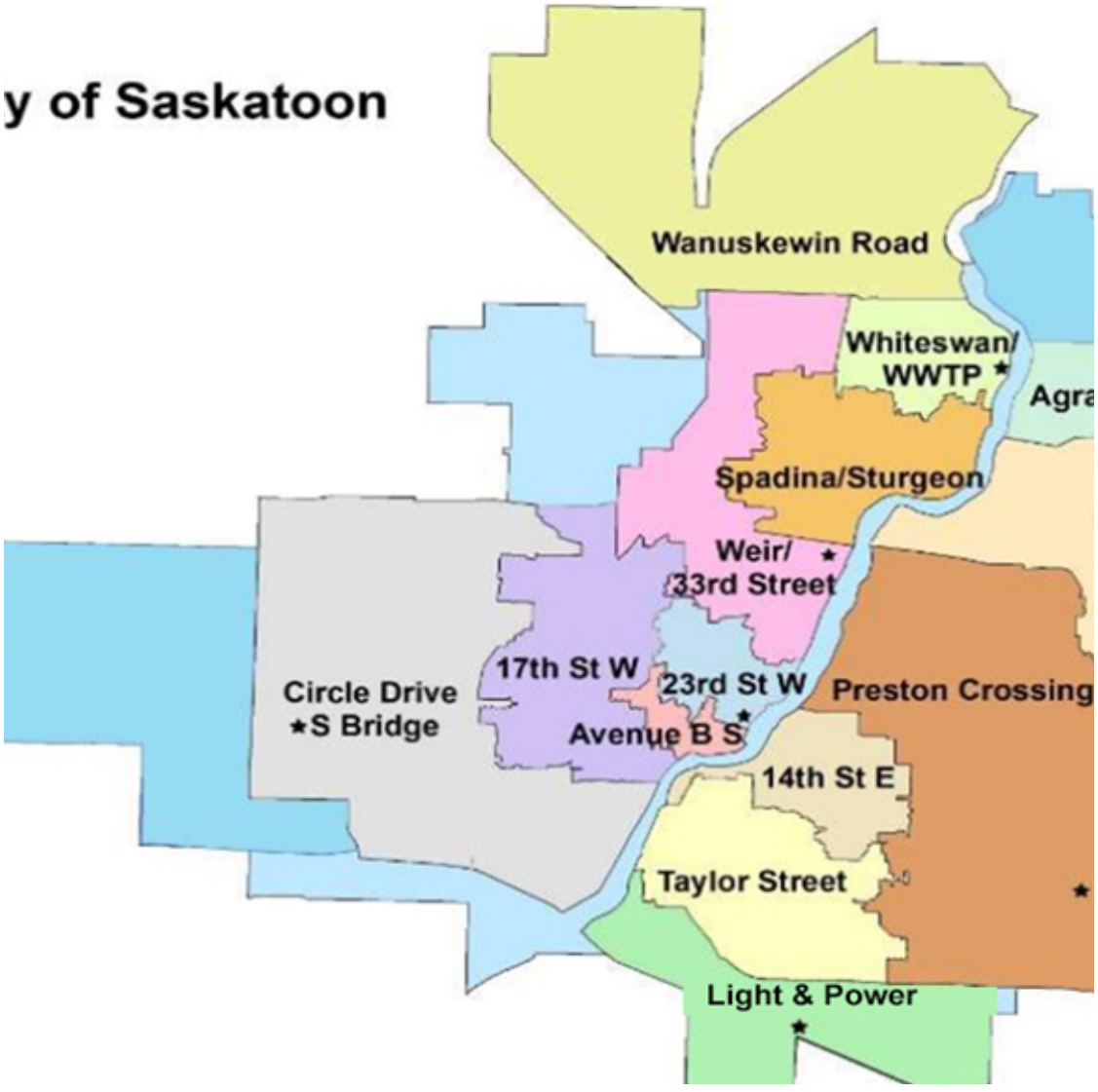

0

N
a Road
Dog Park

1.25
2.5
5 Kilometers

Supplementary information B2: Precipitati

Preciptation data from: https://www.wunderground.com/weather/ca/saskatoon

S. Circle Dr. Bridge E

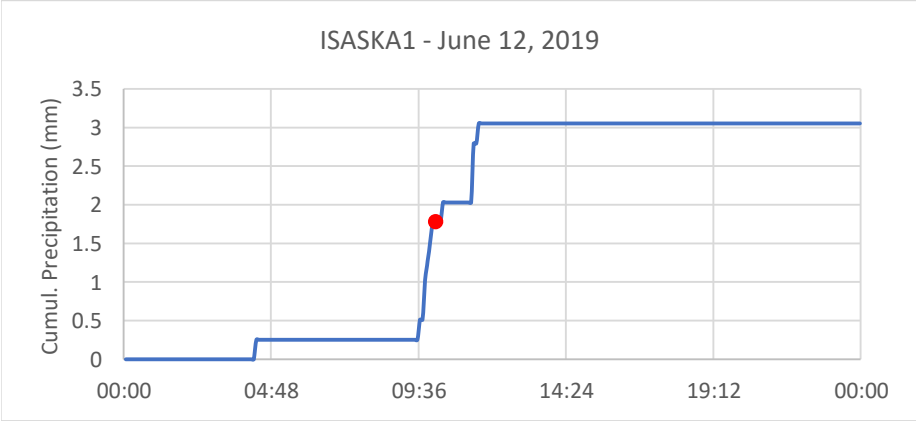

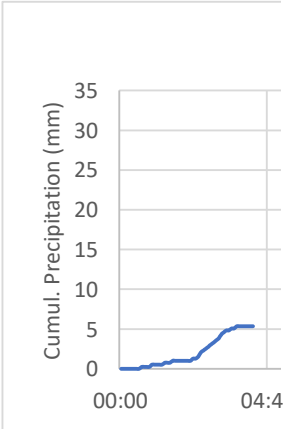

S. Circle Dr. Bridge W

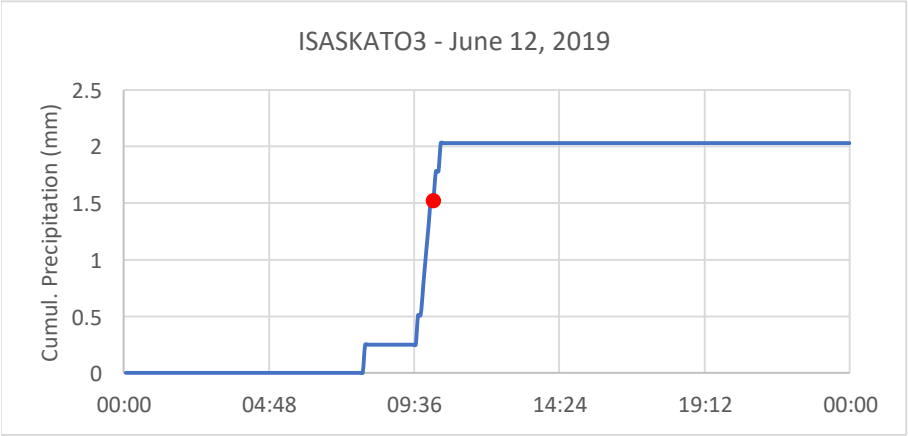

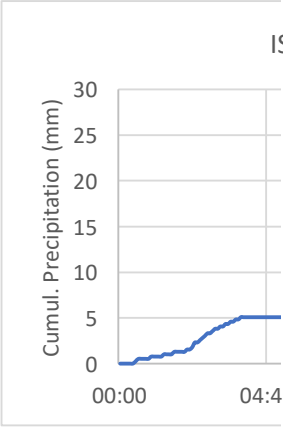

MacPherson Ave.

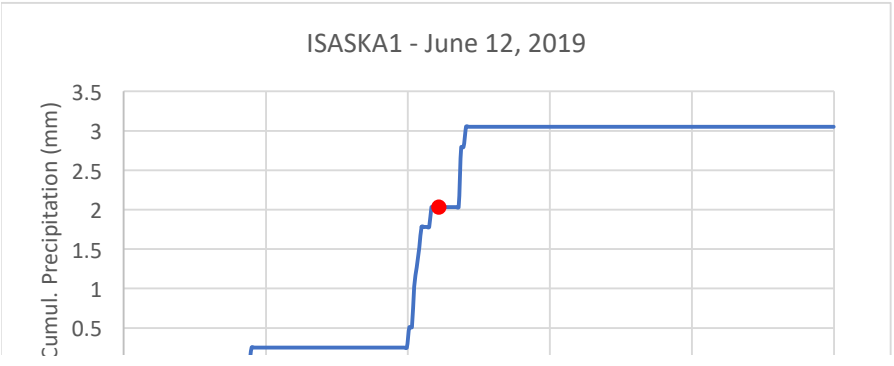

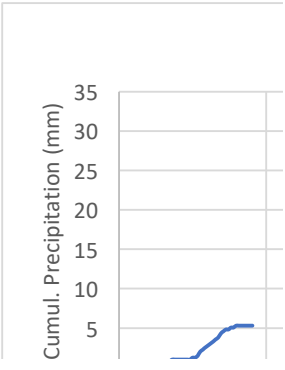

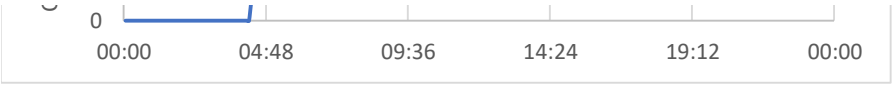

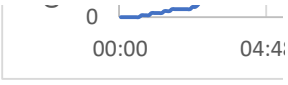

14th St. E

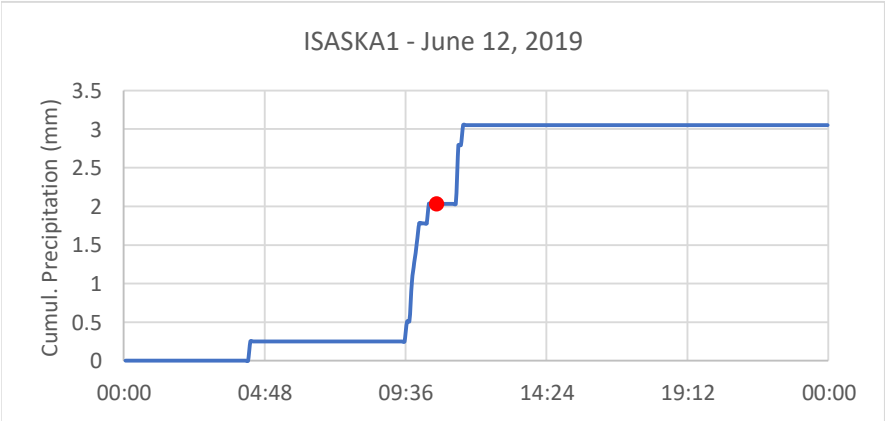

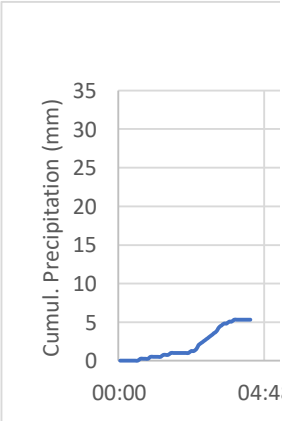

17th St. W

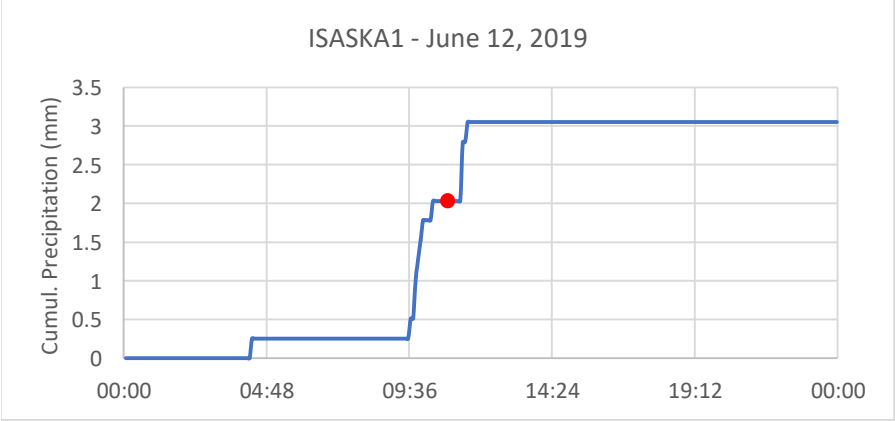

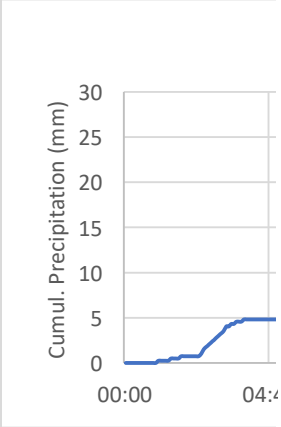

23rd St. W

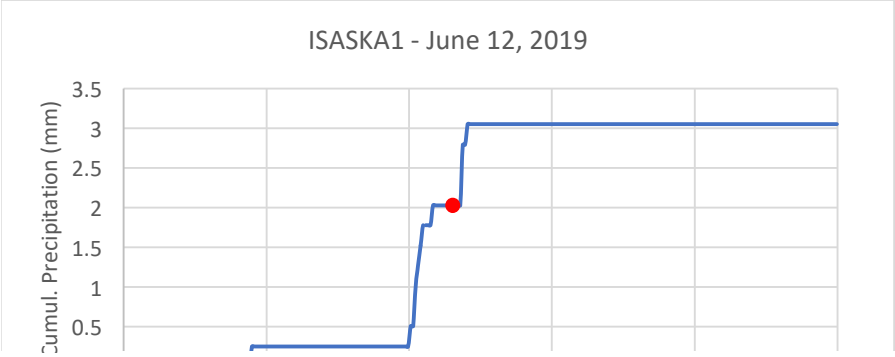

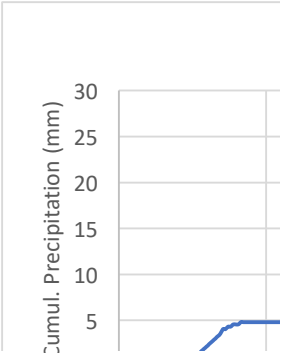

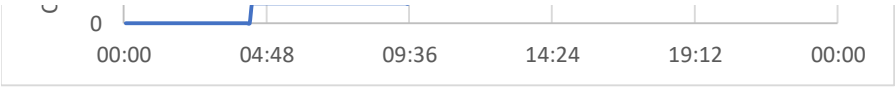

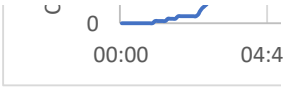

Silverwood Dog Park

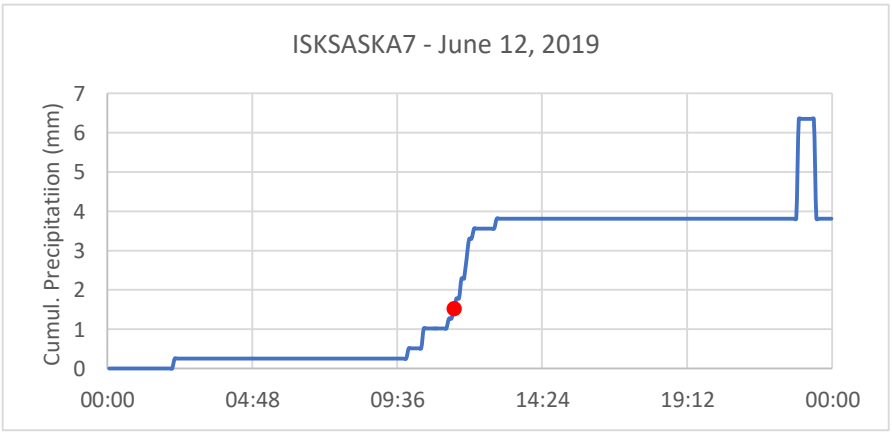

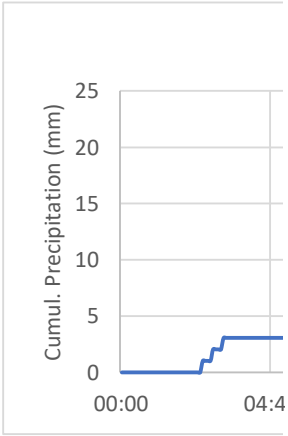

on events and sampling time (red dots) of s

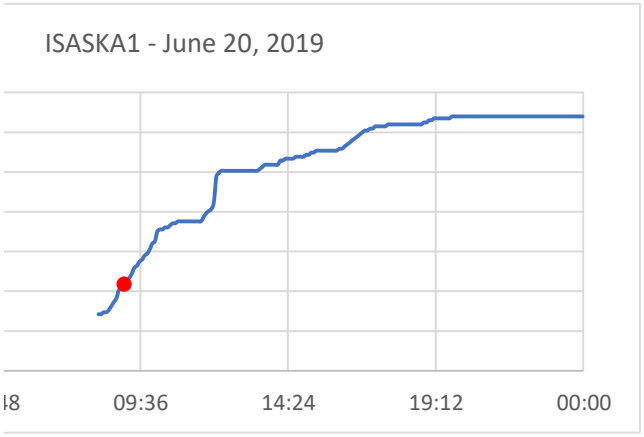

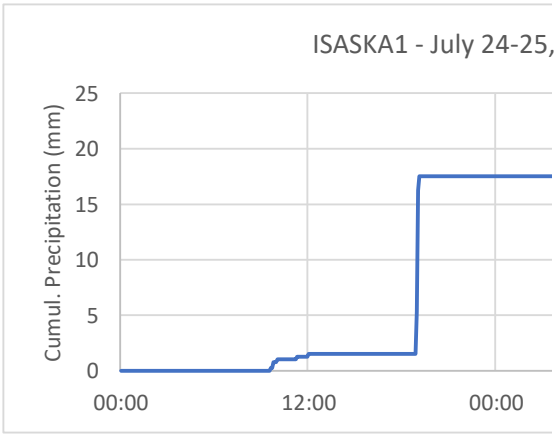

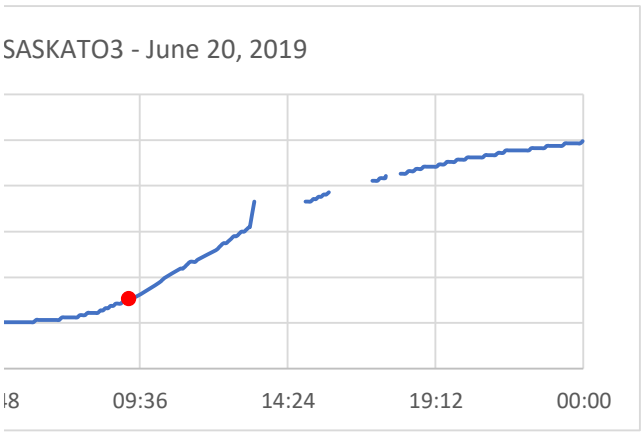

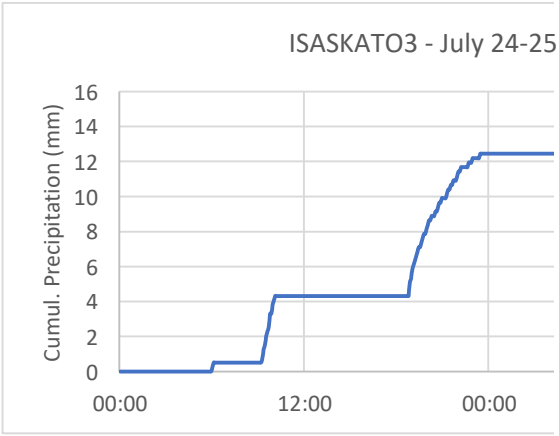

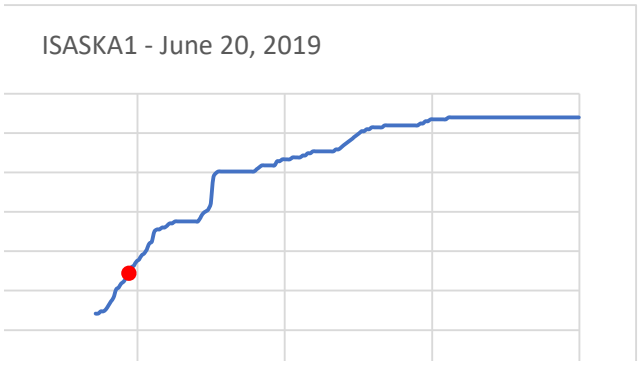

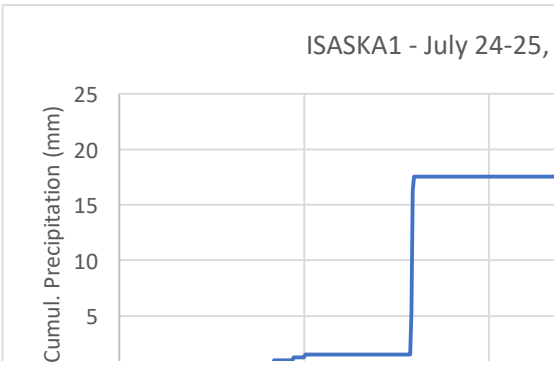

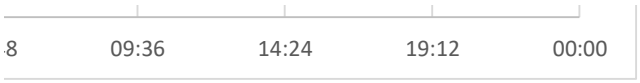
8
09:36
14:24
19:12
00:00

0
00:00
12:00
00:00

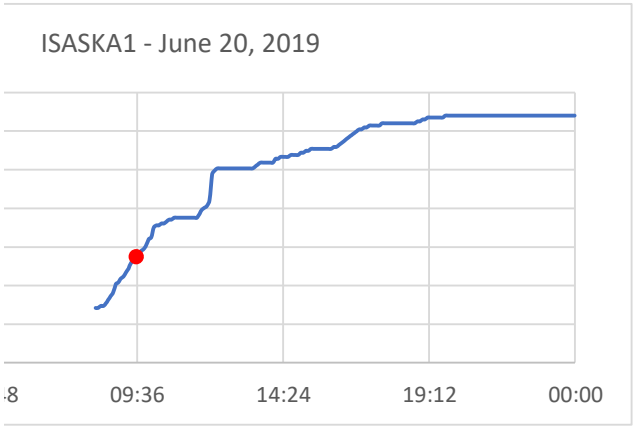
ISASKA1 - June 20, 2019
8
09:36
14:24
19:12
00:00

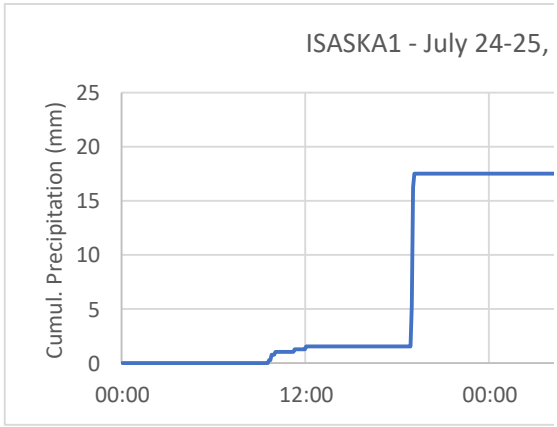
ISASKA1 - July 24-25,
Cumul. Precipitation (mm)
25
20
15
10
5
0
00:00
12:00
00:00

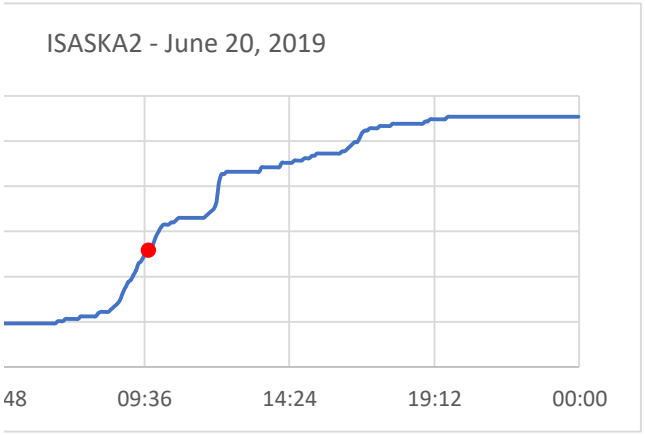
ISASKA2 - June 20, 2019
48
09:36
14:24
19:12
00:00

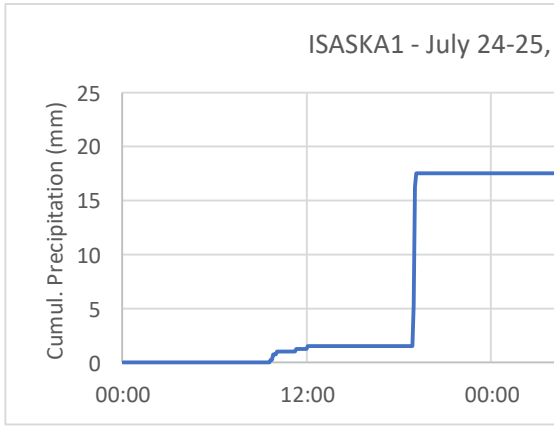
ISASKA1 - July 24-25,
Cumul. Precipitation (mm)
25
20
15
10
5
0
00:00
12:00
00:00

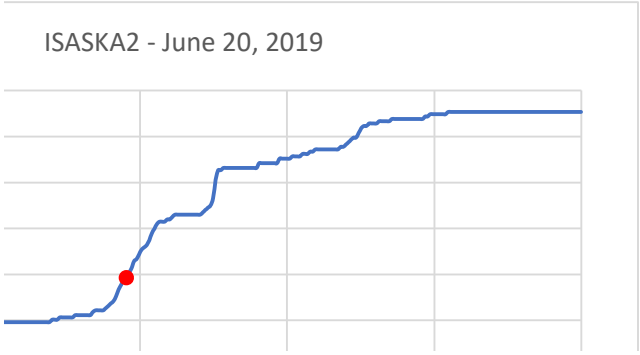
ISASKA2 - June 20, 2019

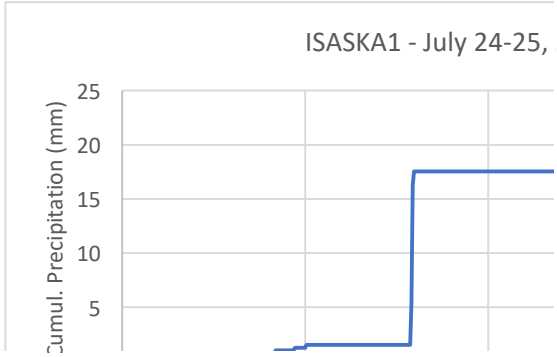
ISASKA1 - July 24-25,
Cumul. Precipitation (mm)
25
20
15
10
5

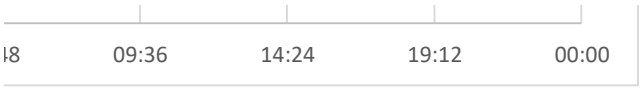
48
09:36
14:24
19:12
00:00

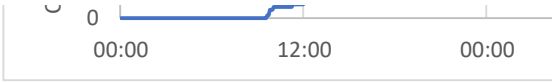
0
00:00
12:00
00:00

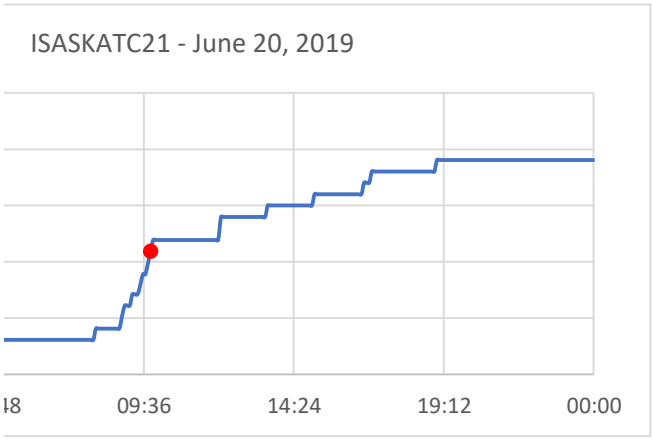
ISASKATC21 - June 20, 2019
48
09:36
14:24
19:12
00:00

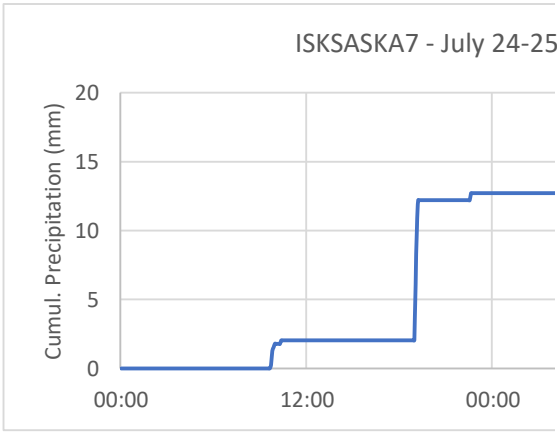
ISKSASKA7 - July 24-25
Cumul. Precipitation (mm)
20
15
10
5
0
00:00
12:00
00:00

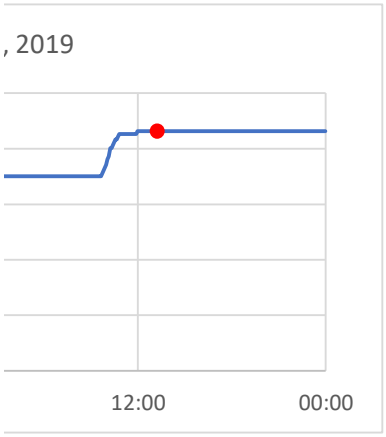
, 2019
12:00
00:00

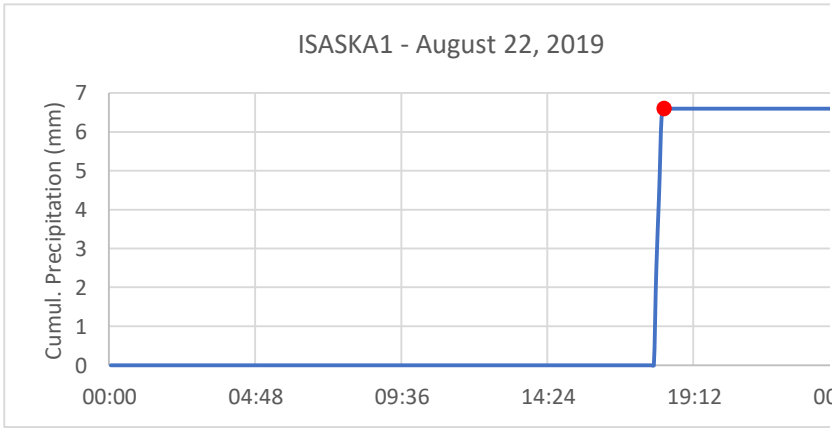
ISASKA1 - August 22, 2019
Cumul. Precipitation (mm)
7
6
5
4
3
2
1
0
00:00
04:48
09:36
14:24
19:12

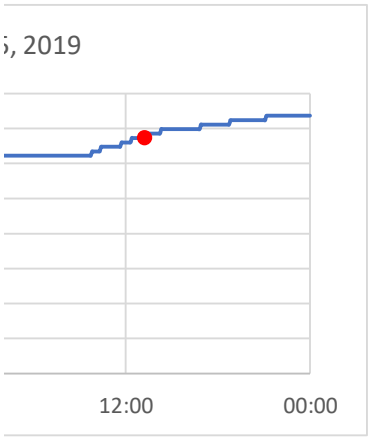
, 2019
12:00
00:00

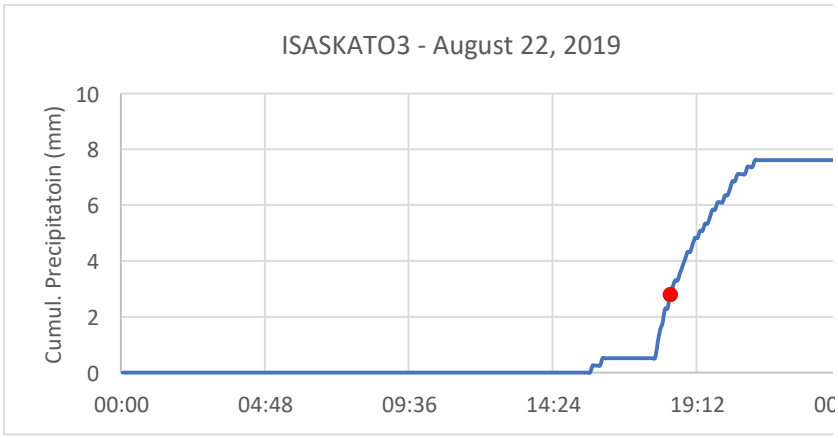
ISASKATO3 - August 22, 2019
Cumul. Precipitatoin (mm)
10
8
6
4
2
0
00:00
04:48
09:36
14:24
19:12

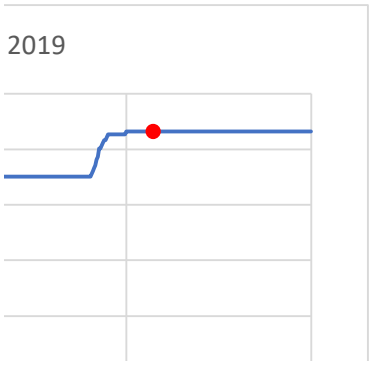
2019

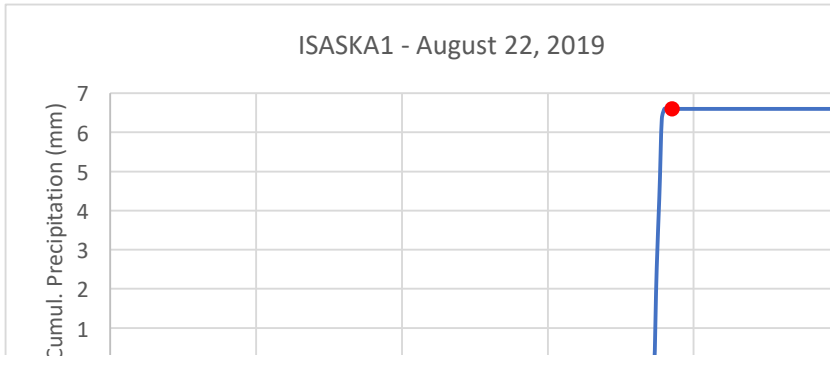
ISASKA1 - August 22, 2019
Cumul. Precipitation (mm)
7
6
5
4
3
2
1

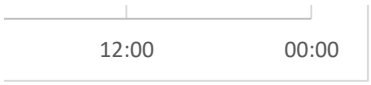
12:00
00:00

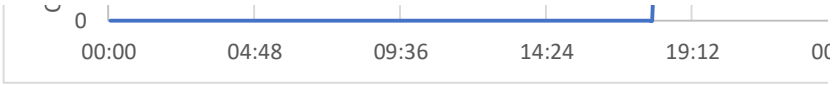
0
00:00
04:48
09:36
14:24
19:12

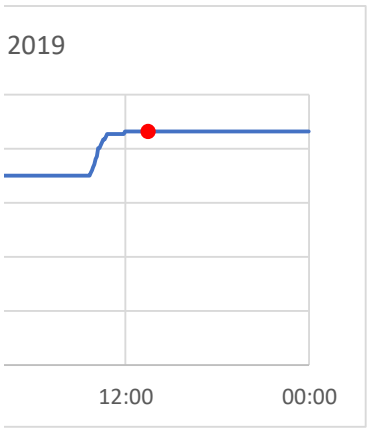
2019
12:00
00:00

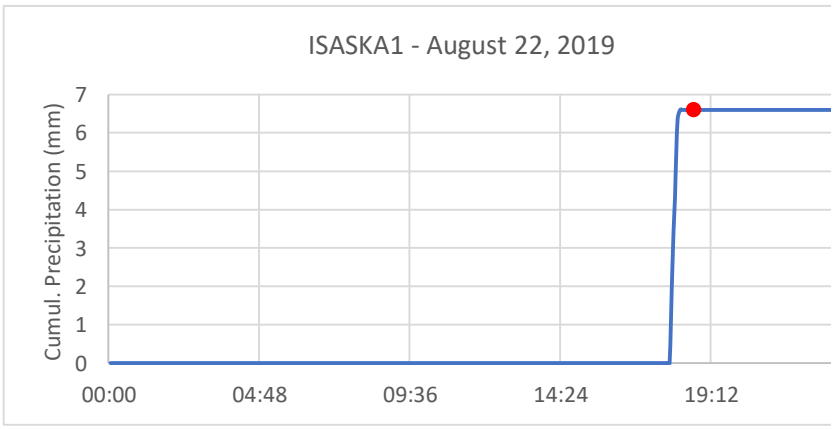
ISASKA1 - August 22, 2019
Cumul. Precipitation (mm)
7
6
5
4
3
2
1
0
00:00
04:48
09:36
14:24
19:12

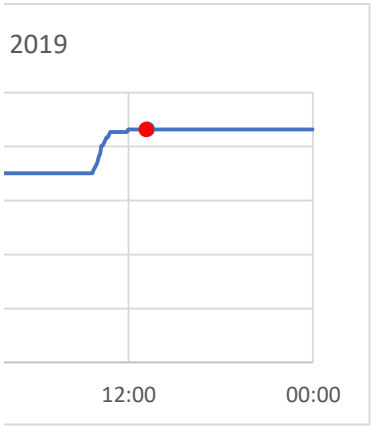
2019
12:00
00:00

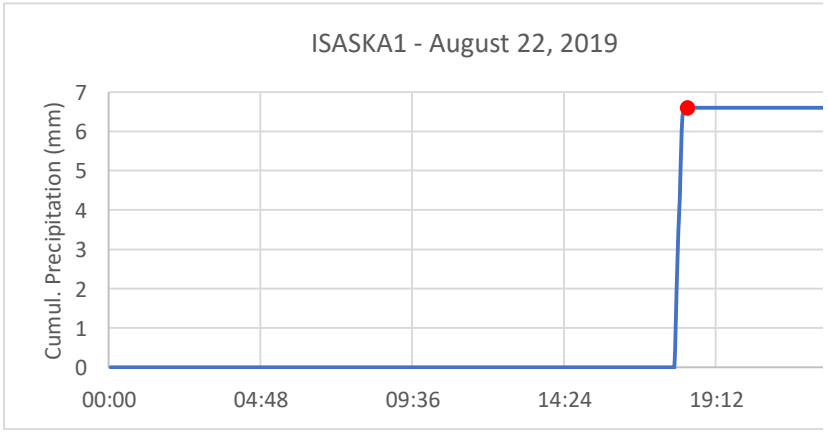
ISASKA1 - August 22, 2019
Cumul. Precipitation (mm)
7
6
5
4
3
2
1
0
00:00
04:48
09:36
14:24
19:12

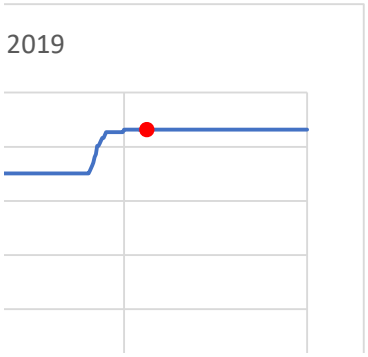
2019

ISASKA1 - August 22, 2019
Cumul. Precipitation (mm)
7
6
5
4
3
2
1

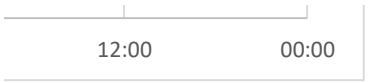
12:00
00:00

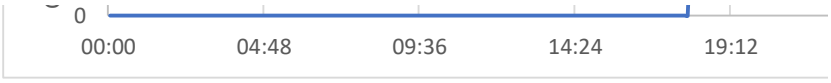
0
00:00
04:48
09:36
14:24
19:12

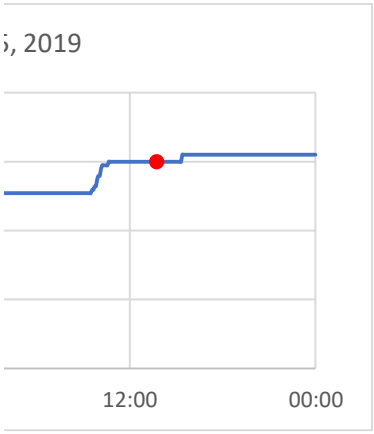
, 2019
12:00
00:00

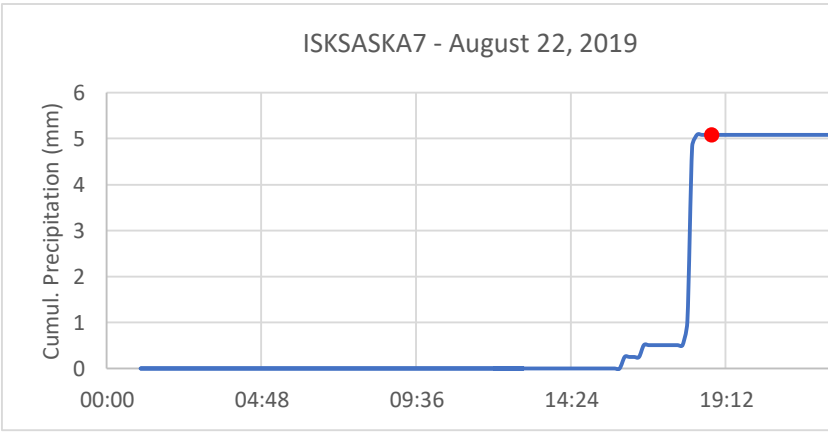
ISKSASKA7 - August 22, 2019
Cumul. Precipitation (mm)
6
5
4
3
2
1
0
00:00
04:48
09:36
14:24
19:12

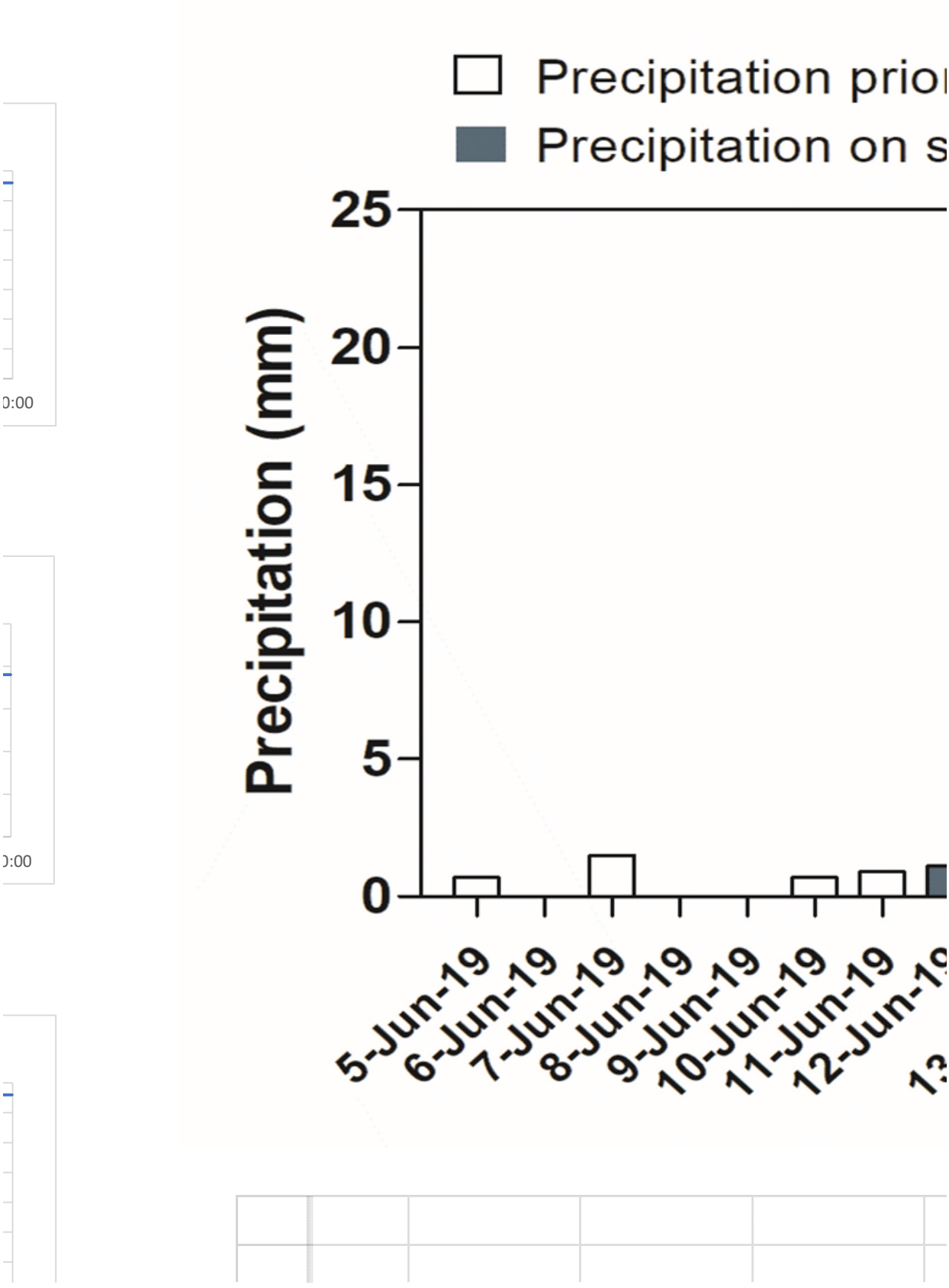
Precipitation prio
Precipitation on s
25
20
15
10
5
0
Precipitation (mm)
5-Jun-19
6-Jun-19
7-Jun-19
8-Jun-19
9-Jun-19
10-Jun-19
11-Jun-19
12-Jun-19

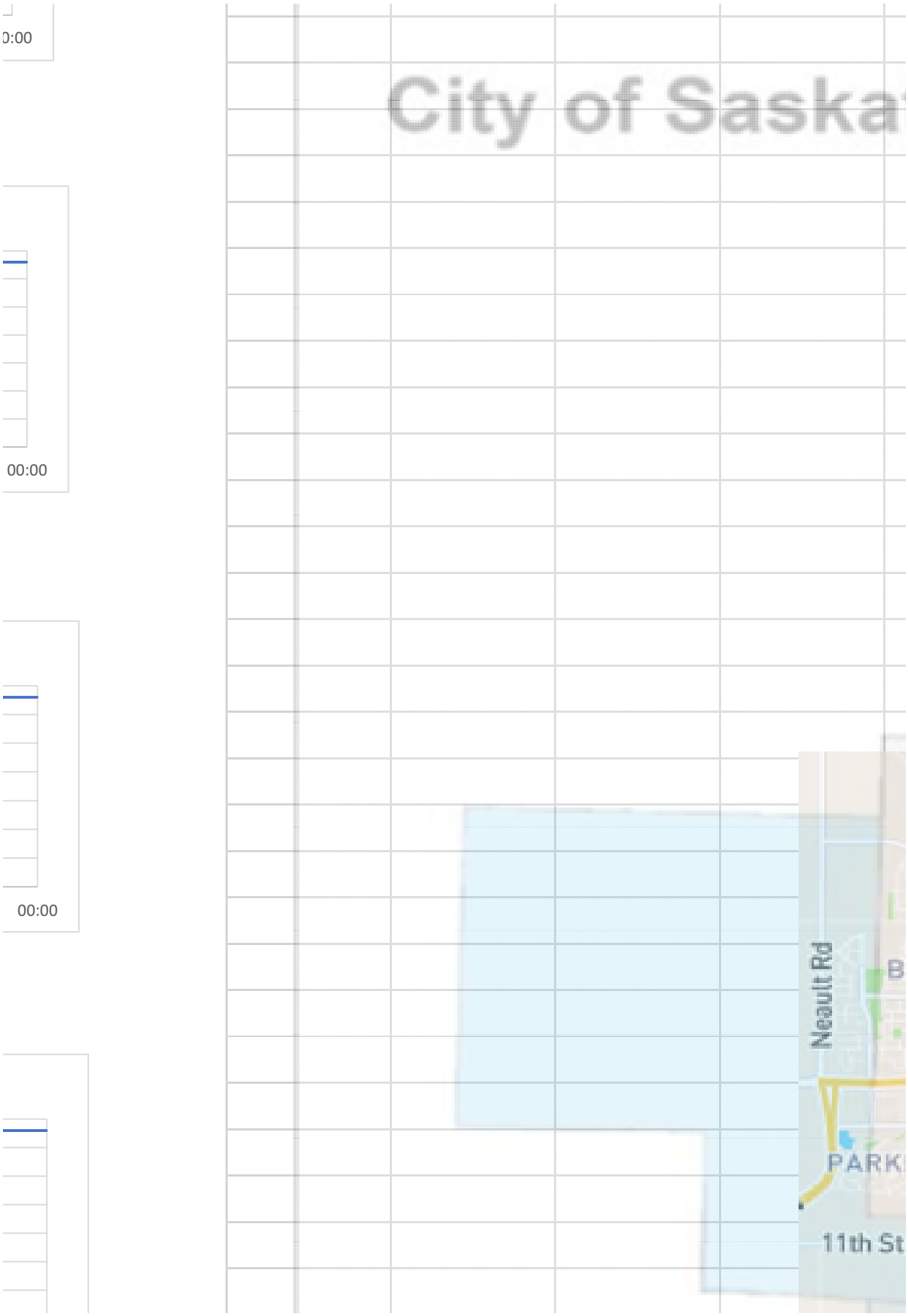
City of Saska
:00
00:00
00:00
Neault Rd
PARK
11th St

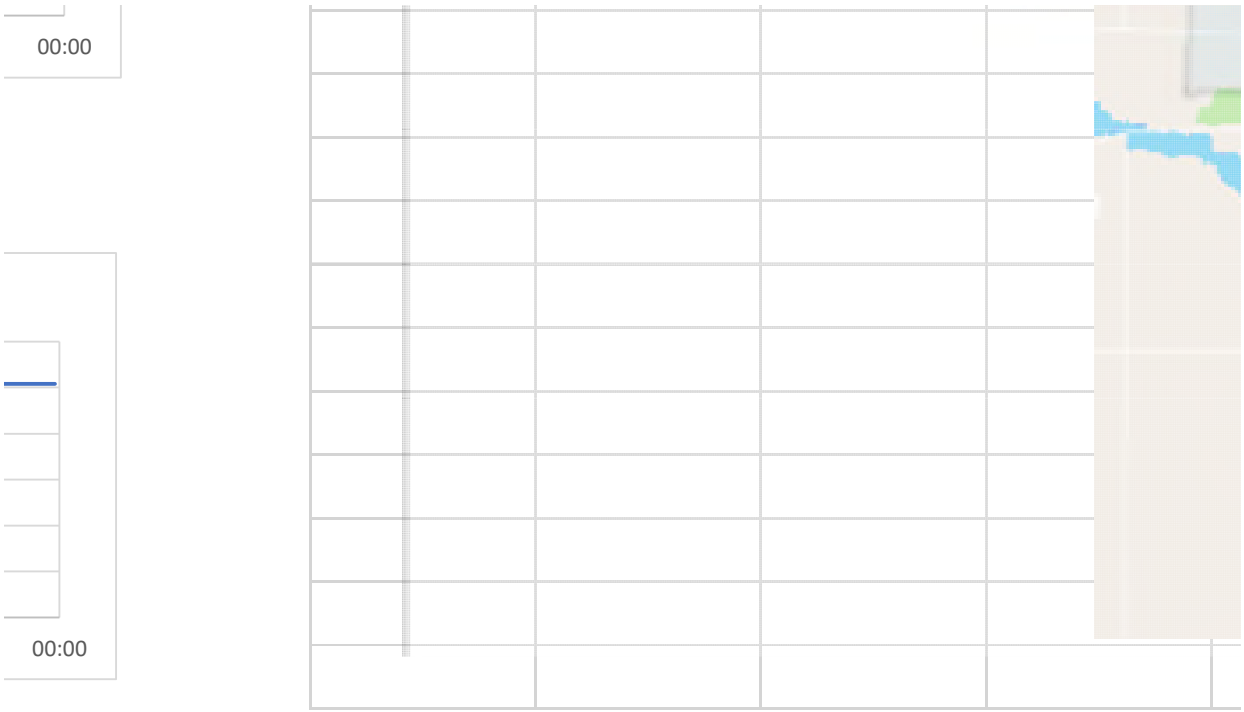
00:00
00:00

r to sampling day

sampling day

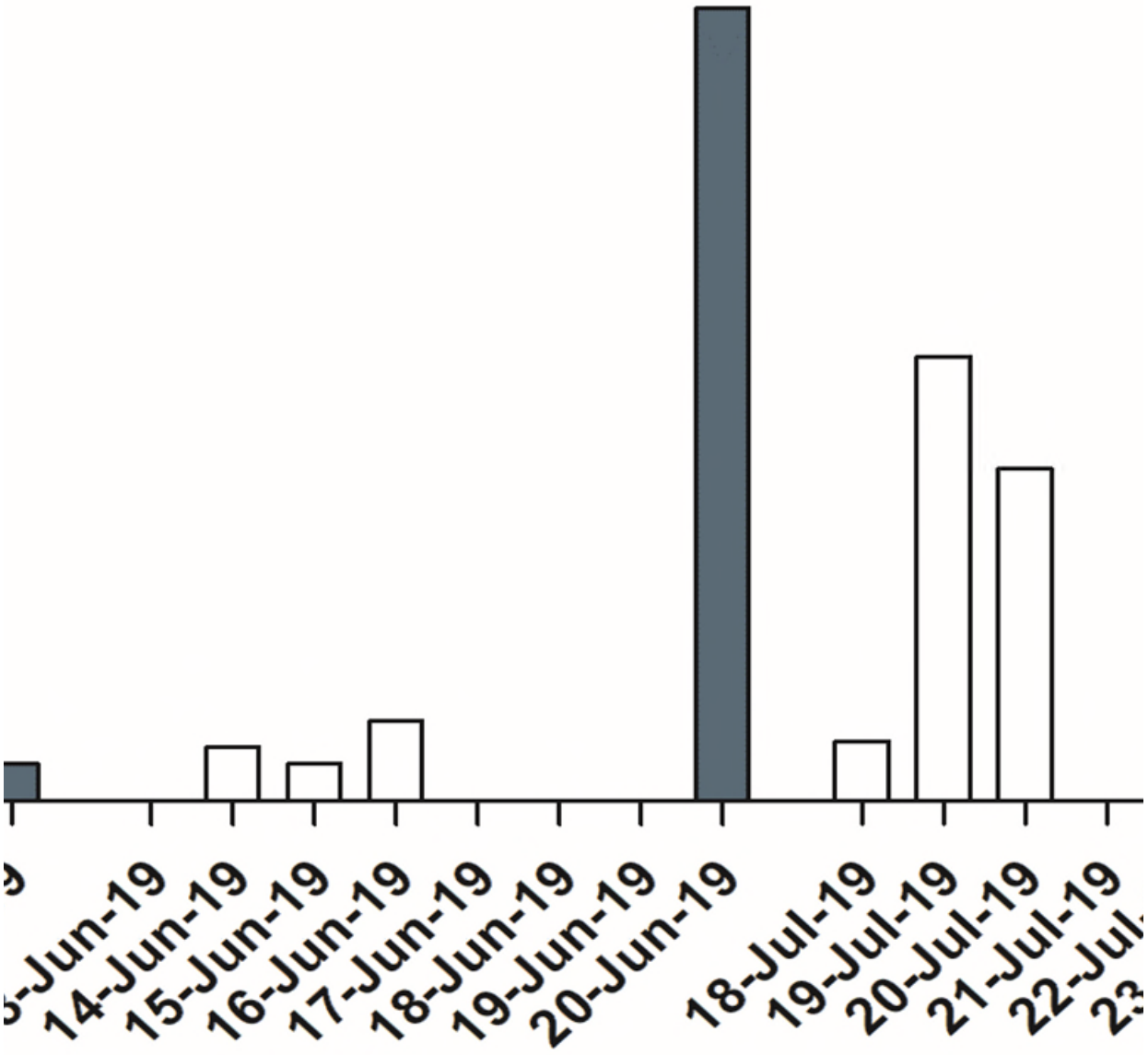

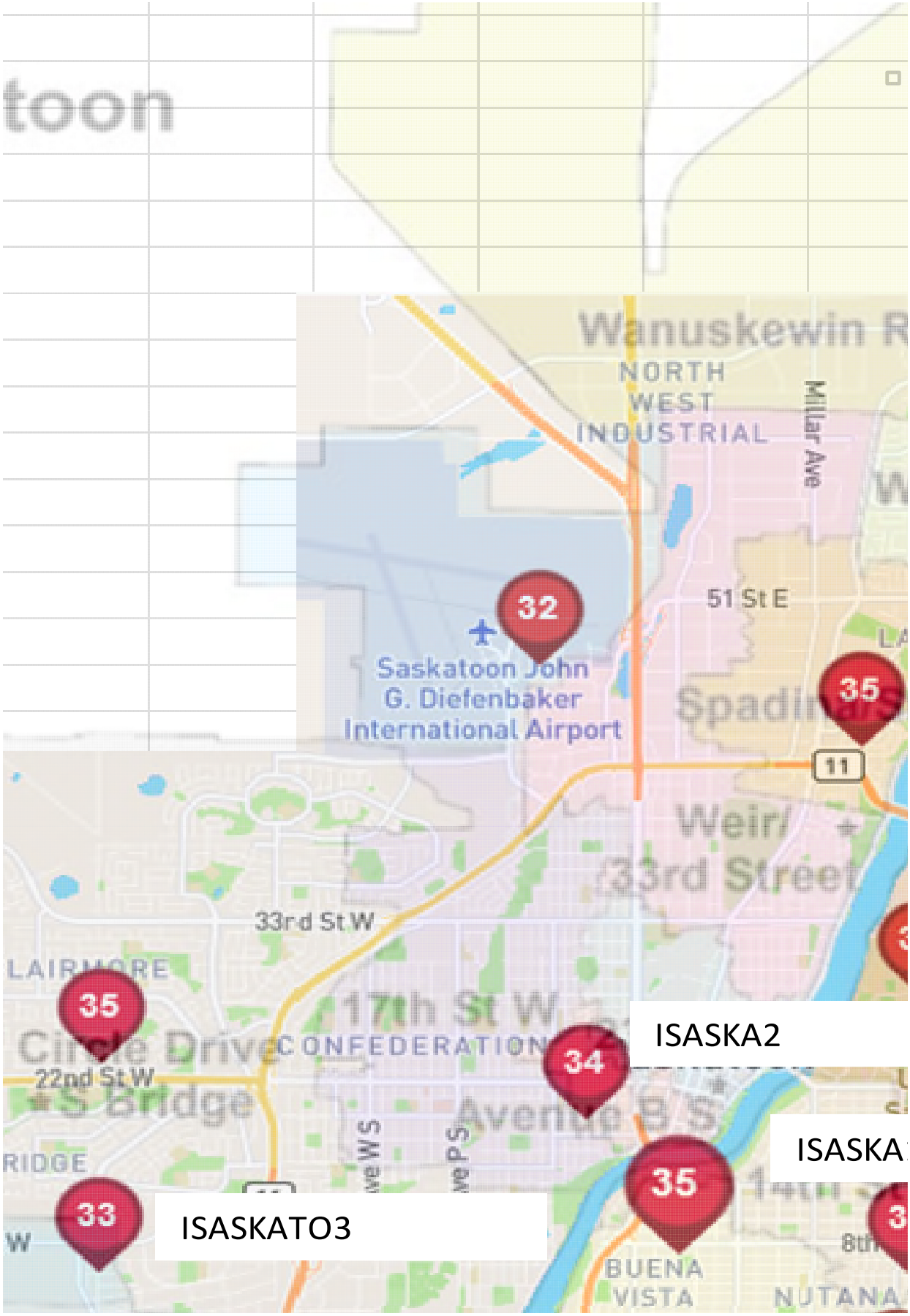
toon
Wanuskewin R
NORTH
WEST
INDUSTRIAL
Miller Ave
51 St E
32
Saskatoon John
G. Diefenbaker
International Airport
35
11
Weir
33rd Street
33rd St W
LAIRMORE
35
17th St W
Circle Drive
CONFEDERATION
34
22nd St W
Avenue B S
RIDGE
35
33
W
BUENA
VISTA
NUTANA
ISASKA2
ISASKA
ISASKATO3

762
11
11
EXHIBITION
Ruth St E
AVALON
WATERFORD
Valley Rd
762
219

-19
-Jul-19
24-Jul-19
25-Jul-19
15-Aug-19
16-Aug-19
17-Aug-19
18-Aug-19
19-Aug-19
20-Aug-19
21-Aug-19
22-Aug-19

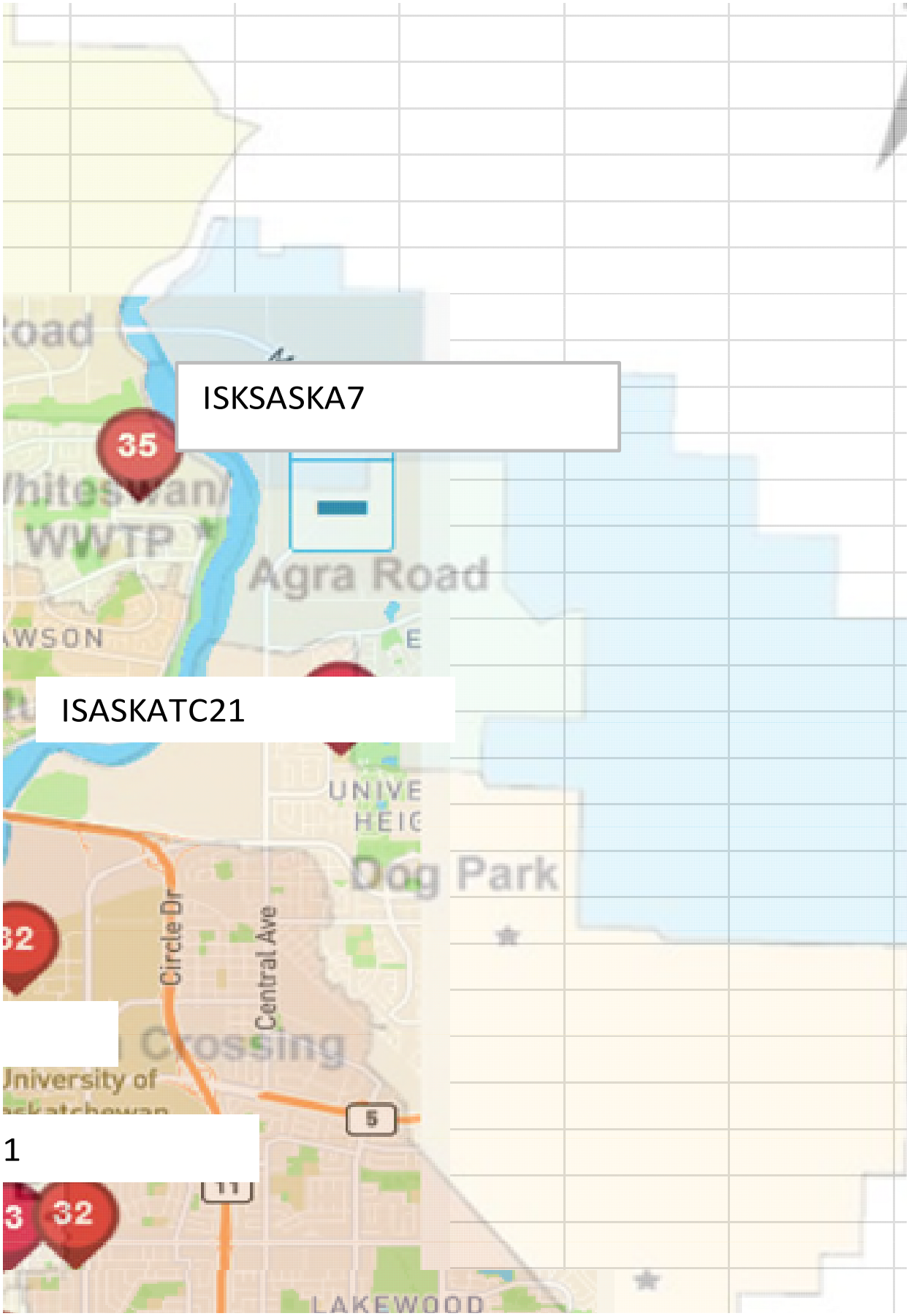
ISKSASKA7
ISASKATC21
1
35
WWTP
Agra Road
Dog Park
Circle Dr
Central Ave
Crossing
University of
5
11
32
LAKEWOOD

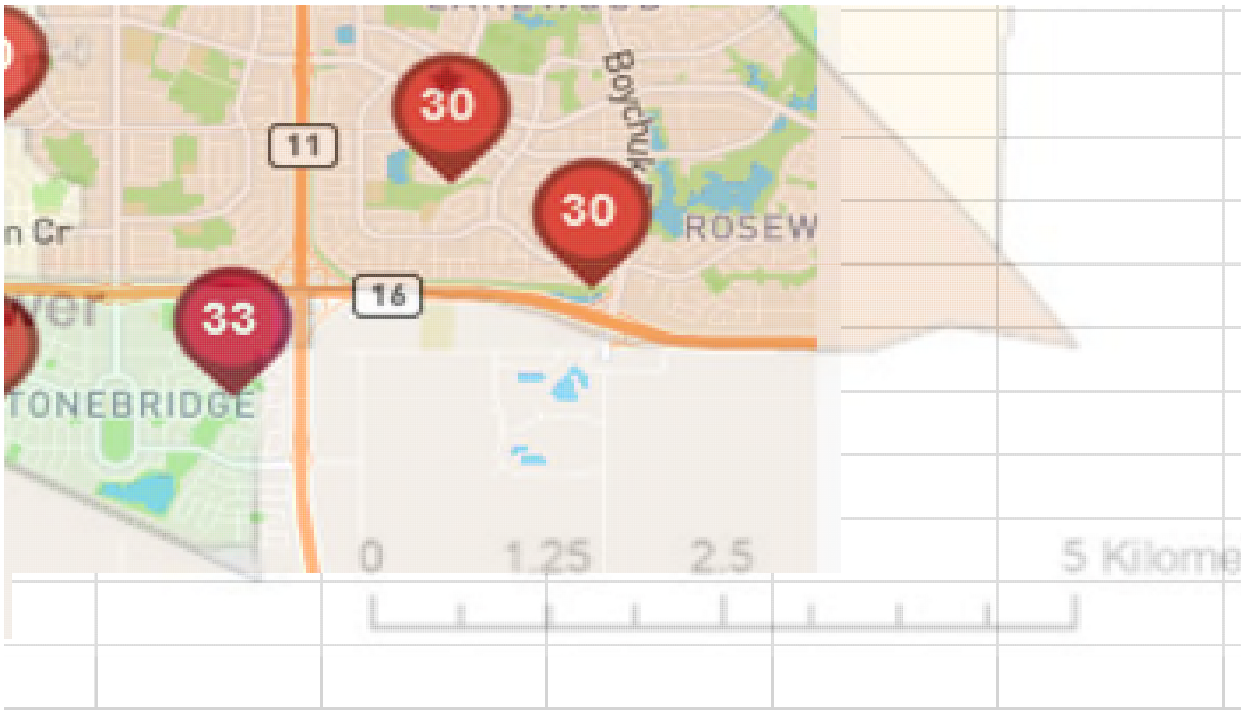
30
11
30
16
33
ROSEW
TONEBRIDGE
0
1.25
2.5
5 Kilome

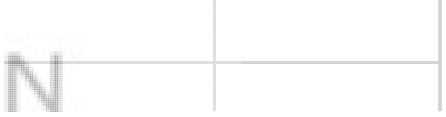

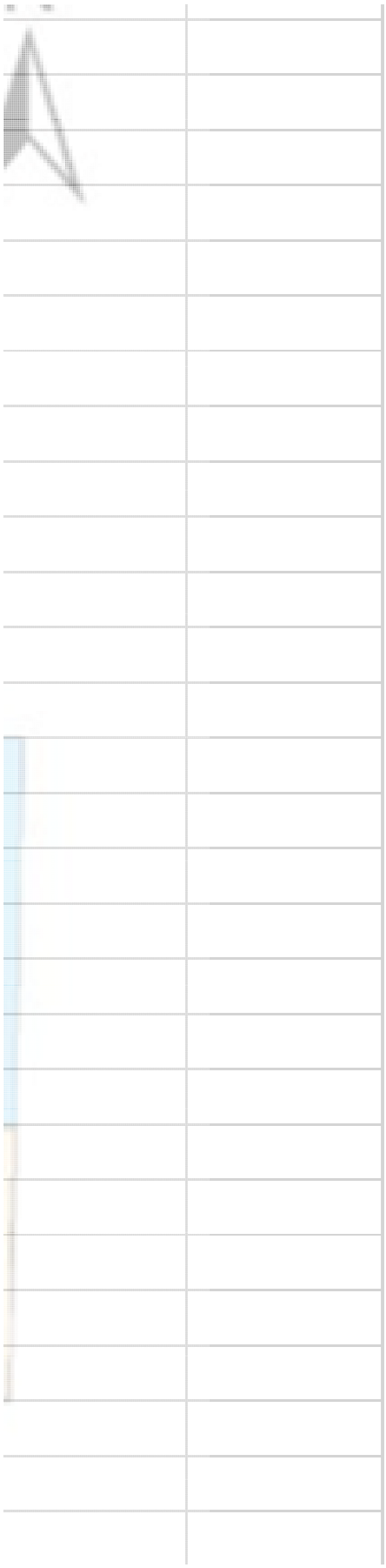

ters	

Supplementary information B3: Concentrations (ng/L) of target compounds in stormwater samples
ND = not detected **NS = not sampled**

6PPD-q	Circle E	Circle W	MacPh	14th St E	17th St W
12-Jun-19	ND	ND	ND	ND	ND
20-Jun-19	235.8	1401.9	212.3	1259.7	887.0
25-Jul-19	103.3	90.8	NS	466.9	NS
22-Aug-19	NS	ND	NS	NS	86.2

DPG	Circle E	Circle W	MacPh	14th St E	17th St W
12-Jun-19	23.4	9.9	25.1	2047.8	955.8
20-Jun-19	3621.2	1868.4	1805.3	52.1	1652.3
25-Jul-19	1112.5	61200.0	NS	187000.0	NS
22-Aug-19	91.6	310.6	241969.5	248000.0	4297.8

DCA	Circle E	Circle W	MacPh	14th St E	17th St W
12-Jun-19	1.1	1.0	ND	59.5	34.3
20-Jun-19	18.7	30.6	12.9	ND	30.9
25-Jul-19	4.3	11.8	NS	60.7	NS
22-Aug-19	NS	7.3	NS	NS	44.9

DCU	Circle E	Circle W	MacPh	14th St E	17th St W
12-Jun-19	78.3	62.7	140.6	550.4	287.0
20-Jun-19	509.4	298.8	207.9	ND	389.7
25-Jul-19	222.6	1376.5	NS	3232.3	NS
22-Aug-19	NS	102.3	NS	NS	104.8

CPU	Circle E	Circle W	MacPh	14th St E	17th St W
12-Jun-19	ND	ND	ND	395.3	178.7
20-Jun-19	76.5	224.5	88.7	22.3	296.6
25-Jul-19	41.4	44.7	NS	175.2	NS
22-Aug-19	NS	32.4	NS	NS	30.0

Supplementary information B3: Loadings (kg) of targe

ND = not detected **NS = not sampled**

23rd St E	Silverwood	6PPD-q	Circle E	Circle W
ND	ND	**12-Jun-19**	ND	ND
1097.4	1162.2	**20-Jun-19**	235.8	1401.9
NS	NS	**25-Jul-19**	103.3	90.8
115.6	ND	**22-Aug-19**	NS	ND

23rd St E	Silverwood	DPG	Circle E	Circle W
ND	438.6	**12-Jun-19**	23.4	9.9
1939.1	324.6	**20-Jun-19**	3621.2	1868.4
364249.8	363328.0	**25-Jul-19**	1112.5	61200.0
4822.8	135.7	**22-Aug-19**	91.6	310.6

23rd St E	Silverwood	DCA	Circle E	Circle W
ND	29.3	**12-Jun-19**	1.1	1.0
40.8	29.6	**20-Jun-19**	18.7	30.6
NS	NS	**25-Jul-19**	4.3	11.8
76.2	ND	**22-Aug-19**	NS	7.3

23rd St E	Silverwood	DCU	Circle E	Circle W
ND	225.8	**12-Jun-19**	78.3	62.7
407.7	210.0	**20-Jun-19**	509.4	298.8
NS	NS	**25-Jul-19**	222.6	1376.5
168.7	6.7	**22-Aug-19**	NS	102.3

23rd St E	Silverwood	CPU	Circle E	Circle W
ND	139.6	**12-Jun-19**	ND	ND
282.1	119.4	**20-Jun-19**	76.5	224.5
NS	NS	**25-Jul-19**	41.4	44.7
60.1	1.9	**22-Aug-19**	NS	32.4

et compounds in stormwater samples

	MacPh	14th St E	17th St W	23rd St E	Silverwood
ND	ND	ND	ND	ND	
212.3	1259.7	887.0	1097.4	1162.2	
NS	466.9	NS	NS	NS	
NS	NS	86.2	115.6	ND	

	MacPh	14th St E	17th St W	23rd St E	Silverwood
25.1	2047.8	955.8	ND	438.6	
1805.3	52.1	1652.3	1939.1	324.6	
NS	187000.0	NS	364249.8	363328.0	
241969.5	248000.0	4297.8	4822.8	135.7	

	MacPh	14th St E	17th St W	23rd St E	Silverwood
ND	59.5	34.3	ND	29.3	
12.9	ND	30.9	40.8	29.6	
NS	60.7	NS	NS	NS	
NS	NS	44.9	76.2	ND	

	MacPh	14th St E	17th St W	23rd St E	Silverwood
140.6	550.4	287.0	ND	225.8	
207.9	ND	389.7	407.7	210.0	
NS	3232.3	NS	NS	NS	
NS	NS	104.8	168.7	6.7	

	MacPh	14th St E	17th St W	23rd St E	Silverwood
ND	395.3	178.7	ND	139.6	
88.7	22.3	296.6	282.1	119.4	
NS	175.2	NS	NS	NS	
NS	NS	30.0	60.1	1.9	

Supplementary information B4: Concentrations (ng/L) of target compounds in snowmelt samples
ND = not detected NS = not sampled

6PPD-q	Valley Rd		USask		Central Ave	
2-Apr-19	NS		422.4	NS		
13-Apr-19	421.1		756.0	NS		
18-Apr-19	396.9		604.3	NS		
24-Apr-19	NS		362.4		249.6	
7-Mar-20	NS		80.5	NS		
26-Mar-20	148.9	NS		NS		
29-Mar-20	65.9	NS		NS		
10-Apr-20	29.3	NS		NS		
17-Apr-20	ND		15.2	NS		
20-Apr-20	140.0	NS		NS		
23-Apr-20	ND		22.8	ND		
28-Apr-20	105.7		53.7		36.5	
1-May-20	164.3	NS		NS		
5-May-20	NS		171.8		128.9	
12-May-20	118.3		25.6	NS		

DPG	Valley Rd		USask		Central Ave	
2-Apr-19	NS		1851.2	NS		
13-Apr-19	729.8		1215.8	NS		
18-Apr-19	391.6		932.3	NS		
24-Apr-19	NS		713.3		492.9	
7-Mar-20	NS		1283.3	NS		
26-Mar-20	422.2	NS		NS		
29-Mar-20	1155.3	NS		NS		
10-Apr-20	213.4	NS		NS		
17-Apr-20	603.7		564.3	NS		
20-Apr-20	467.3	NS		NS		
23-Apr-20	381.8		416.2		639.0	
28-Apr-20	1935.5		217.9	ND		
1-May-20	619.9	NS		NS		
5-May-20	NS		1251.5		464.1	
12-May-20	8666.6		306.5	NS		

DCA	Valley Rd		USask		Central Ave	
2-Apr-19	NS		5.7	NS		
13-Apr-19	6.1		23.0	NS		
18-Apr-19	6.7		7.0	NS		
24-Apr-19	NS		5.8		3.5	
7-Mar-20	NS		8.4	NS		
26-Mar-20	ND	NS		NS		
29-Mar-20	ND	NS		NS		
10-Apr-20	2.1	NS		NS		
17-Apr-20	3.3		2.0	NS		

20-Apr-20		3.4	NS		NS		
23-Apr-20	ND		ND				5.3
28-Apr-20	ND		ND		ND		
1-May-20		3.6	NS		NS		
5-May-20	NS		ND				2.8
12-May-20		3.8		3.5	NS		

DCU	**Valley Rd**		**USask**		**Central Ave**	
2-Apr-19	NS		168.9	NS		
13-Apr-19	ND		102.5	NS		
18-Apr-19	ND	ND		NS		
24-Apr-19	NS	ND		ND		
7-Mar-20	NS		58.7	NS		
26-Mar-20	ND	NS		NS		
29-Mar-20	ND	NS		NS		
10-Apr-20	ND	NS		NS		
17-Apr-20	ND		44.3	NS		
20-Apr-20	ND	NS		NS		
23-Apr-20		14.3	9.6			1.6
28-Apr-20	ND	ND		ND		
1-May-20	ND	NS		NS		
5-May-20	NS	ND				124.7
12-May-20		29.2	20.0	NS		

CPU	**Valley Rd**		**USask**		**Central Ave**	
2-Apr-19	NS		179.6	NS		
13-Apr-19		54.1	217.1	NS		
18-Apr-19		34.9	64.7	NS		
24-Apr-19	NS		39.0			46.4
7-Mar-20	NS		7.2	NS		
26-Mar-20	ND	NS		NS		
29-Mar-20		2.6	NS	NS		
10-Apr-20		5.4	NS	NS		
17-Apr-20		10.0	ND	NS		
20-Apr-20		2.3	NS	NS		
23-Apr-20		4.8	ND			2.6
28-Apr-20	ND	ND				13.5
1-May-20		3.0	NS	NS		
5-May-20	NS	ND				65.3
12-May-20		5.9	4.5	NS		

	Wanuskewin	
NS		
	73.7	
	235.7	
	145.4	
NS		
NS		
NS		
NS		
	29.2	
NS		
NS		
	49.0	
NS		
NS		
	110.7	
	Wanuskewin	
NS		
	645.6	
	597.6	
	113.3	
NS		
NS		
NS		
NS		
	119.3	
NS		
NS		
	358.0	
NS		
NS		
	2005.5	
	Wanuskewin	
NS		
	8.5	
	5.8	
	4.3	
NS		
NS		
NS		
NS		
	3.9	

NS
NS
3.5
NS
NS
ND

Wanuskewin

NS
ND
ND
ND
NS
NS
NS
NS
42.4
NS
NS
ND
NS
NS
27.2

Wanuskewin

NS
15.5
56.5
15.6
NS
NS
NS
NS
2.4
NS
NS
8.9
NS
NS
3.4